hemato

MDPI

Review

Precision Immunopathology in Classic Hodgkin Lymphoma: From Conventional Pathology to Integrated Biologic Profiling

Antonino Carbone [1,*], Chiara Costanza Volpi [2], Desirè Viola Trupia [2] and Annunziata Gloghini [2,†]

[1] Centro di Riferimento Oncologico, Istituto di Ricovero e Cura a Carattere Scientifico, National Cancer Institute, 33081 Aviano, Italy
[2] Department of Advanced Pathology, Fondazione IRCCS Istituto Nazionale dei Tumori, 20133 Milan, Italy; chiara.volpi@istitutotumori.mi.it (C.C.V.); desire.trupia@istitutotumori.mi.it (D.V.T.); annunziata.gloghini@istitutotumori.mi.it (A.G.)
* Correspondence: acarbone@cro.it
† Annunziata Gloghini is a Former Senior Scientist of the Department of Advanced Pathology, Fondazione IRCCS Istituto Nazionale dei Tumori, 20133 Milan, Italy.

Abstract

Classic Hodgkin lymphoma (cHL) is histologically defined by rare Hodgkin and Reed–Sternberg (HRS) cells embedded within an extensive, biologically active immune microenvironment that HRS cells actively recruit and reprogram to sustain their own survival. For decades, diagnosis has relied on morphology and a limited immunohistochemical panel (CD30, CD15, PAX5, CD20, EBER), an approach that confirms disease identity but provides little insight into the immune ecosystem that governs prognosis and treatment response. Over the past fifteen years, discovery of near-universal 9p24.1/*CD274-PDCD1LG2-JAK2* copy-number alterations, CIITA gene fusions, B2M mutations, and NF-κB/JAK-STAT pathway activation has progressively reframed cHL—conceptually rather than through a formal reclassification—as a genetically driven disorder of immune evasion. In parallel, multiplex immunohistochemistry, imaging mass cytometry, digital spatial profiling, spatial transcriptomics, single-cell sequencing, whole-slide digital pathology, and machine-learning algorithms now allow the tumor-immune ecosystem to be mapped at unprecedented resolution. This convergence is giving rise to what we term "precision immunopathology": an overarching conceptual framework, rather than a formal diagnostic category, that combines morphology with immune, molecular, spatial, and computational data and that, once prospectively validated, may refine prognostic stratification, prediction of benefit from PD-1 blockade and other immunotherapies, and non-invasive disease monitoring through circulating tumor DNA. At present, beyond the standard diagnostic panel, no tissue biomarker is required to select patients for PD-1 blockade or CD30-directed therapy. This review summarizes the evolution from conventional to precision immunopathology in cHL, discusses the technologies enabling this transition, grades each candidate biomarker and assay by level of evidence and clinical readiness (routine, clinically validated but non-routine, or investigational), incorporates the move of PD-1 blockade into first-line therapy (SWOG S1826) and the BrECADD regimen (HD21), proposes a minimum dataset for an integrated precision immunopathology report, and discusses the practical barriers—tissue availability, cost, turnaround time, standardization, and regulatory validation—that must be overcome before an ecosystem-centered diagnostic model can be translated into routine hematopathology practice.

Check for updates

Academic Editor: David Sallman

Received: 18 September 2026
Revised: 9 October 2026
Accepted: 20 October 2026
Published: 22 October 2026

Copyright: © 2026 by the authors. Licensee MDPI, Basel, Switzerland. This article is an open access article distributed under the terms and conditions of the Creative Commons Attribution (CC BY) license.

Keywords: tumor microenvironment; immune evasion; immune checkpoint inhibitors; B7-H1 antigen; major histocompatibility complex; biomarkers; tumor; circulating tumor DNA; spatial analysis; artificial intelligence; precision medicine

1. Introduction

Classic Hodgkin lymphoma (cHL) is a B-cell-derived lymphoid neoplasm characterized by a strikingly small population of malignant Hodgkin and Reed–Sternberg (HRS) cells—typically about 1–5% of the cellularity of the involved tissue [1,2]—surrounded by a florid, reactive infiltrate of T cells, B cells, macrophages, eosinophils, plasma cells, and stromal elements [3,4]. This numerical paradox, in which a minority neoplastic population coexists with, and actively depends upon, an overwhelming reactive background, has long framed cHL as a paradigmatic model of tumor-microenvironment interdependence within oncology more broadly [3]. Epidemiologically, cHL shows a bimodal age distribution and remains one of the most curable lymphoid malignancies with modern combination chemotherapy, yet a clinically meaningful subset of patients relapse or become primary refractory, and others are over-treated relative to their true risk, underscoring the need for biomarkers that anticipate treatment failure—or unnecessary toxicity—before either occurs [5,6].

For most of its diagnostic history, cHL pathology has been "tumor-centered": the pathologist identifies HRS cells by morphology, confirms lineage and subtype with a standard immunohistochemical panel, and assigns a histological subtype according to the World Health Organization (WHO) classification of lymphoid neoplasms [7–9] or, more recently, the International Consensus Classification (ICC) [10]. This approach is robust for establishing a diagnosis—and for separating cHL from its biologically distinct relative, nodular lymphocyte-predominant Hodgkin lymphoma, which has been recognized as a distinct entity for decades on the basis of its divergent immunophenotype and clinical behavior and has recently been re-designated nodular lymphocyte-predominant B-cell lymphoma by the ICC [9,10]—but it is largely blind to the biological features—antigen presentation status, checkpoint expression, spatial immune architecture, genomic alterations—that determine why some tumors respond durably to a given therapy while others progress despite an apparently identical morphological picture.

The clinical stakes of this diagnostic blind spot are not trivial. Frontline combination chemotherapy, typically anthracycline-based, cures the large majority of newly diagnosed patients regardless of histological subtype, yet clinicians currently have few tools beyond baseline clinical risk scores and interim imaging to identify, at diagnosis, which patients truly need treatment intensification and which could be safely spared additional toxicity [5,6]. A biopsy-based assay capable of resolving the same information that interim positron-emission tomography currently provides only after one or two cycles of chemotherapy—or of identifying, up front, patients whose tumor biology predicts primary resistance to standard chemotherapy but exquisite sensitivity to checkpoint blockade—would meaningfully change how this disease is risk-stratified and treated from the outset.

Conventional prognostic stratification in cHL is based almost exclusively on clinical and imaging parameters. In early-stage disease, risk factors defined by the major cooperative groups (German Hodgkin Study Group, EORTC/LYSA, and NCCN)—including a large mediastinal mass, elevated erythrocyte sedimentation rate, B symptoms, extranodal involvement, and the number of involved nodal areas—separate favorable from unfavorable disease and guide treatment intensity [5,6]. In advanced-

stage disease, the International Prognostic Score (IPS) combines seven factors (serum albumin < 4 g/dL, hemoglobin < 10.5 g/dL, male sex, age ≥ 45 years, stage IV disease, leukocytosis ≥ 15×10^9/L, and lymphocytopenia < 0.6×10^9/L or <8% of white cells) [11]; because its discriminatory power has declined with contemporary therapy, it has recently been refined by the Advanced-Stage Hodgkin Lymphoma International Prognostic Index (A-HIPI), which models continuous clinical variables [12] and has been externally validated within the GHSG HD21 trial [13]. Functional imaging adds baseline total metabolic tumor volume (MTV) [14] and, above all, interim positron emission tomography–computed tomography (PET-CT) response assessed by the Deauville scale, which currently underpins response-adapted treatment [15,16]. None of these tools, however, directly captures the biology of the HRS cell or of its microenvironment.

Over the last decade and a half, a series of discoveries has repositioned cHL as a disease actively sculpted by, and actively sculpting, its immune microenvironment. Genomic and fluorescence in situ hybridization (FISH)-based analyses demonstrated recurrent copy-number alterations of the 9p24.1 locus—present in nearly all cases, most often as relative copy gain and, in about one-third of cases, as amplification—which contains CD274 (encoding PD-L1), PDCD1LG2 (encoding PD-L2), and JAK2, providing a genetic basis for the near-universal overexpression of PD-1 ligands that helped rationalize checkpoint-inhibitor therapy in this disease [17,18]. Complementary work identified recurrent CIITA gene fusions that transcriptionally silence MHC class II expression [19] and B2M mutations that abrogate MHC class I presentation [20], revealing convergent, HRS-cell-intrinsic strategies of antigen-presentation escape layered onto a chronically active NF-κB signaling background that itself cooperates with JAK/STAT pathway activation to sustain the malignant phenotype [4,21]. Of note, this reframing did not result from a single formal redefinition of the disease: it emerged progressively from these landmark genomic studies, published between 2010 and 2019 [17–20,22,23], whereas both the WHO classification and the ICC still define cHL on morphologic and immunophenotypic grounds [9,10]. These molecular insights have been paralleled by an equally rapid expansion of technologies capable of resolving the spatial architecture of the immune infiltrate—multiplex immunohistochemistry and immunofluorescence, including cyclic immunofluorescence [1,24], imaging mass cytometry [25], digital spatial profiling [26,27], spatial transcriptomics [2,28,29], and single-cell approaches such as mass cytometry and single-cell RNA sequencing [30,31]—alongside whole-slide digital pathology [32] and machine-learning tools [33–35] that may quantify and integrate these layers with greater reproducibility than manual assessment, although their clinical value remains to be established.

The convergence of molecular pathology, spatial biology, digital pathology, and artificial intelligence is transforming cHL diagnostics from a tumor-centered exercise into what we term "precision immunopathology". We use this expression as an overarching conceptual framework—not as an established or formally recognized diagnostic category—to denote an ecosystem-centered approach that integrates the malignant clone with its immune and stromal context to support diagnosis, prognosis, treatment prediction, and disease monitoring (Table 1, Figure 1). This review is organized around the principal diagnostic domains through which this transition is occurring—conventional morphology and immunohistochemistry, immune and checkpoint profiling, spatial immunopathology, molecular pathology, and digital pathology with artificial intelligence—before considering which of these layers currently inform clinical decision-making, which remain investigational, and what practical barriers must be overcome before they can be integrated into routine practice. Throughout the review, and in Tables 2–8, biomarkers and assays are classified into three levels of clinical readiness: (i) established routine diagnostic biomarkers; (ii) clinically validated but non-routine biomarkers, supported by trial-embedded or

independently validated data but not required for treatment decisions; and (iii) investigational or emerging technologies, whose value has so far been shown only in discovery or retrospective cohorts. We also consistently distinguish between diagnostic, prognostic (associated with outcome irrespective of therapy), and predictive (associated with benefit from a specific therapy) biomarkers.

This review builds on, but is distinct from, our previous syntheses, each of which focused on a single biological or technological domain: the contribution of the tumor microenvironment to checkpoint-inhibitor therapy [36], immune checkpoint molecules in Hodgkin lymphoma and other hematological malignancies [37], the morphology, phenotype, genotype, and cell of origin of HRS cells [38], artificial intelligence in cHL [39], and predictors of sensitivity to immune therapies [40]. The distinctive contribution of the present work is diagnostic and operational: it (i) integrates these domains into a single, tiered diagnostic framework centered on the pathology report; (ii) grades each candidate biomarker and assay according to the clinical question addressed, level of evidence, feasibility on routine formalin-fixed, paraffin-embedded (FFPE) material, turnaround time, availability of standardized scoring, and potential to change treatment decisions (Table 6); (iii) proposes a minimum dataset for an integrated precision immunopathology report (Table 7); and (iv) translates it into a scenario-based testing algorithm that specifies a core panel for every case, the clinical scenarios that warrant additional analyses, and the results expected to change management (Table 8); and (v) discusses the practical barriers to implementation and the clinical populations in which the framework may need adaptation. Overlap with our earlier reviews has been kept to the minimum necessary for a self-contained synthesis, and readers are referred to them for in-depth discussion of individual domains.

Table 1. Precision immunopathology in classic Hodgkin lymphoma: from conventional pathology to integrated biological profiling *.

From Conventional Pathology	To Precision Immunopathology	Current Capability and Clinical Status	Anticipated Benefit (Requires Prospective Validation)
Morphological diagnosis and disease classification	Integrated biological characterization of the tumor and immune ecosystem	Diagnosis and classification: routine	Refined prognosis, treatment prediction, and disease monitoring
Identification of Hodgkin and Reed–Sternberg (HRS) cells and histological subtype	Morphology integrated with immune, molecular, and spatial profiling	Morphology and standard IHC: routine	More comprehensive disease characterization
Limited immunohistochemistry (e.g., CD30, CD15, PAX5, CD20, EBER)	Multiparametric assessment of immune checkpoints, antigen presentation, immune-cell composition, macrophage polarization, stromal remodeling, and spatial organization	Investigational; not required for treatment selection (Table 6)	Identification of immune escape mechanisms and therapeutic vulnerabilities
Spatial analysis: Qualitative evaluation of tissue architecture	Multiplex IHC/IF, cyclic immunofluorescence, digital spatial profiling, imaging mass cytometry, and spatial transcriptomics	Research use only (investigational)	Characterization of immune-cell neighborhoods and functional tissue organization
Molecular pathology: Selected ancillary molecular tests	Integration of FISH, NGS, transcriptomics, single-cell technologies, and ctDNA	9p24.1 FISH and targeted NGS: investigational; ctDNA: clinically validated, non-routine (Table 6)	Identification of recurrent genomic alterations (e.g., 9p24.1, *B2M*, *CIITA*, JAK/STAT, NF-κB), biologically relevant subgroups, and non-invasive monitoring
Digital pathology: Visual microscopic evaluation	Whole-slide imaging and quantitative digital pathology	WSI: routine in some centers; quantitative analysis: investigational	Standardized and reproducible biomarker assessment

Table 1. *Cont.*

From Conventional Pathology	To Precision Immunopathology	Current Capability and Clinical Status	Anticipated Benefit (Requires Prospective Validation)
Artificial intelligence (AI): Not routinely incorporated	Machine-learning algorithms integrating histological, molecular, radiological, and clinical data	Investigational; no cHL-specific tool approved	Decision support, predictive modeling, and reduction of observer variability
Overall approach: Tumor-centered pathology	Ecosystem-centered pathology integrating malignant cells with the tumor microenvironment	Conceptual framework	Foundation for precision immunopathology and personalized medicine

* This table provides a conceptual overview; readiness tiers, level of evidence, and supporting references for individual biomarkers and assays are given in Table 6. "Current capability and clinical status" refers to routine practice as of 2026; benefits listed as anticipated require prospective validation. Abbreviations: ctDNA, circulating tumor DNA; FISH, fluorescence in situ hybridization; IF, immunofluorescence; IHC, immunohistochemistry; NGS, next-generation sequencing; WSI, whole-slide imaging.

Literature Search and Selection

This narrative review is based on a literature search of PubMed/MEDLINE, Scopus, and Web of Science covering January 2000 to August 2026; seminal earlier studies were included when they established concepts still in current use. Search terms combined "classic(al) Hodgkin lymphoma" or "Hodgkin Reed-Sternberg cell" with topic-specific terms, including "tumor microenvironment", "PD-L1", "9p24.1", "MHC class I", "MHC class II", "B2M", "CIITA", "macrophages", "multiplex immunohistochemistry", "multiplex immunofluorescence", "imaging mass cytometry", "digital spatial profiling", "spatial transcriptomics", "single-cell", "circulating tumor DNA", "digital pathology", "artificial intelligence", "deep learning", "nivolumab", "pembrolizumab", and "brentuximab vedotin". Reference lists of relevant articles were hand-searched. Priority was given to (i) primary studies in cHL, particularly prospective clinical trials and their correlative biomarker analyses; (ii) large retrospective cohorts with independent validation; (iii) meta-analyses and systematic reviews; and (iv) classification documents. Narrative reviews were used mainly for context. Congress abstracts were considered only for practice-relevant, trial-embedded biomarker data not yet published in full, and are identified as such. Only English-language articles were included. Because the selection was not systematic, some selection bias cannot be excluded; to mitigate it, conflicting or negative results were actively sought for each biomarker discussed

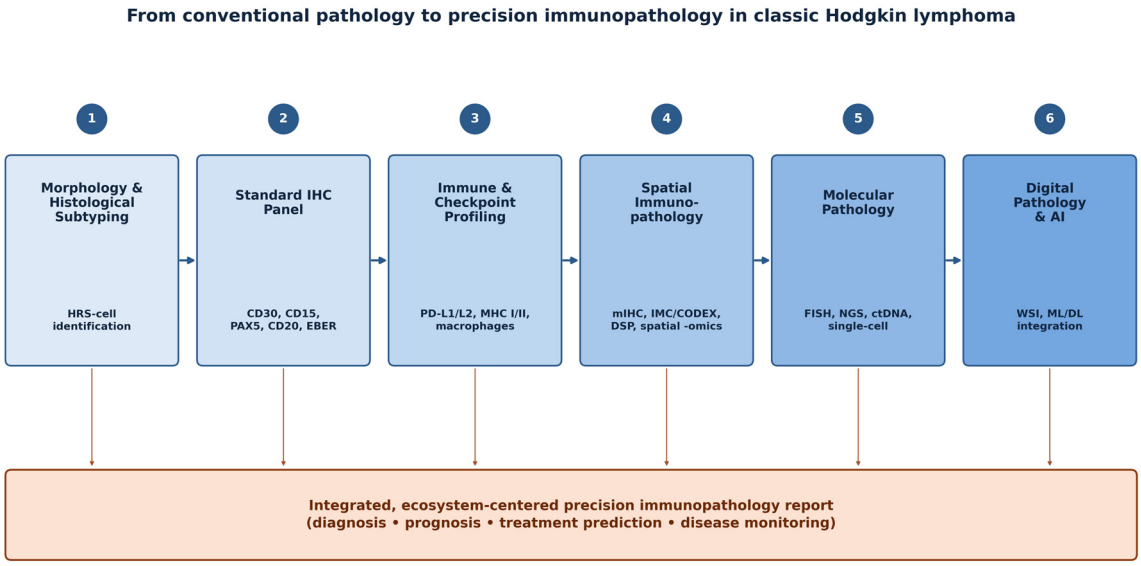


Figure 1. Conceptual evolution of cHL diagnostics from conventional, tumor-centered morphology (boxes 1 and 2: morphology/histological subtyping and the standard immunohistochemical panel)

through four additional layers of biological characterization (boxes 3–6) toward an integrated, ecosystem-centered precision immunopathology report. The six boxes correspond to the five diagnostic domains discussed in the text, conventional morphology and immunohistochemistry being represented by boxes 1 and 2. Only boxes 1 and 2 are currently part of routine diagnostic practice; the integrated report represents a conceptual goal whose prognostic and predictive components require prospective validation.

2. Conventional Pathology: Morphology and Standard Immunohistochemistry

The diagnosis of cHL still begins with recognition of HRS cells: large, often binucleated or multinucleated cells with prominent eosinophilic nucleoli and an "owl-eye" appearance, embedded within a reactive background whose composition varies systematically by histological subtype—nodular sclerosis, mixed cellularity, lymphocyte-rich, and lymphocyte-depleted—as recognized by the current WHO classification [7,9,38]. Because HRS cells frequently lack most B-cell surface markers despite arising from germinal-center B cells, immunophenotyping remains essential to confirm the diagnosis: HRS cells are typically CD30-positive, often CD15-positive, weakly or heterogeneously PAX5-positive, and negative or only weakly positive for CD20 and CD79a [9,41]. In quantitative terms, CD30 is expressed by HRS cells in virtually all cases (a defining feature, with membranous and paranuclear Golgi-type staining); CD15 is positive in approximately 75–85% of cases, often in only a proportion of HRS cells; PAX5 shows weak nuclear positivity—weaker than in reactive B cells—in about 90% of cases; CD20 is detected in about 30–40% of cases, usually in a minority of HRS cells and with variable intensity; and CD79a is expressed less frequently. HRS cells are negative for CD45 and show strong nuclear MUM1/IRF4 expression in nearly all cases [7,9,38]. Loss of the B-cell transcription factors OCT2 and BOB.1, or discordant expression of one without the other, is a well-established feature that helps distinguish cHL from CD30-positive large B-cell lymphomas and anaplastic large-cell lymphoma when morphology alone is ambiguous [41]. EBER in situ hybridization identifies EBV-positive cases, which account for approximately 30–40% of cases in Western countries, with marked variation according to histological subtype (about 75% of mixed cellularity versus 10–40% of nodular sclerosis cases), patient age (higher in children in low-income settings and in older adults), geography, and immune status (nearly all HIV-associated cases) [9,38,42], and which carries independent pathogenetic and, in some series, prognostic significance [43,44].

CD30 itself deserves particular emphasis, not only as a diagnostic marker but as a therapeutic target in its own right: this tumor necrosis factor receptor superfamily member, first characterized on HRS cells, provided the biological rationale for the antibody–drug conjugate brentuximab vedotin, and its signaling biology—including soluble CD30 shedding and bidirectional interaction with CD30-ligand-bearing T cells in the surrounding infiltrate—illustrates how a purely "diagnostic" marker can double as a mechanistic node in the tumor-immune crosstalk addressed throughout this review [45,46]. Because CD30 is expressed by HRS cells by definition, CD30 immunostaining confirms the presence of the target but is not used to select patients for brentuximab vedotin, and no expression threshold has been validated; in CD30-positive non-Hodgkin lymphomas, responses to brentuximab vedotin have been observed across a wide range of CD30 expression levels, including low-level expression [47]. Despite its enduring diagnostic value, this conventional panel, summarized alongside the extended immune and spatial markers discussed below in Table 2, provides essentially no information about the functional state of the surrounding immune infiltrate, the antigen-presentation competence of the tumor cells, or the presence of therapeutically actionable checkpoint pathways—precisely the gap that precision immunopathology aims to close.

Table 2. Standard versus extended immunohistochemical and immune-marker panel in classic Hodgkin lymphoma, with type of evidence and current level of clinical implementation.

Marker/Assay	Conventional Diagnostic Role	Precision-Immunopathology Extension	Type of Evidence and Implementation Level	Ref.
CD30	Diagnostic; expressed by HRS cells in virtually all cases	Target of brentuximab vedotin; expression confirms the target, but no threshold is used for patient selection	Diagnostic: routine. Predictive: not established	[9,45–47]
CD15	Diagnostic lineage-supportive marker (~75–85% of cases)	Component of multiplex panels	Diagnostic: routine	[9,38,41]
PAX5 (weak+)	Confirms B-cell origin (weak in ~90% of cases)	Component of multiplex/digital panels for lineage confirmation	Diagnostic: routine	[9,41]
CD20/CD79a/OCT2/BOB.1	B-cell programme assessment (CD20 in ~30–40%, usually a minority of HRS cells)	Included in multiplex panels for cell-of-origin refinement	Diagnostic: routine	[38,41]
MUM1/IRF4	Strong nuclear positivity in nearly all cases; supports diagnosis	Component of multiplex panels	Diagnostic: routine	[7,38]
EBER (in situ hybridization)	EBV status	Prognostic associations inconsistent across age groups and cohorts; correlates with LMP1 and macrophage/cytokine profile	Diagnostic: routine. Prognostic: inconsistent; not used for treatment selection	[43,44,48]
PD-L1/PD-L2 (IHC on HRS cells)	Not part of standard panel	Reflects 9p24.1 status; supports the therapeutic rationale for PD-1 blockade; higher HRS-cell PD-L1 expression associated with longer PFS after nivolumab	Predictive: exploratory (retrospective, trial-correlative); not required for eligibility—responses also occur with low expression. Investigational	[17,18,49]
β2M/MHC class I (IHC; *B2M* mutation by sequencing)	Not assessed	Loss associated with inferior outcome after chemotherapy in a retrospective series	Prognostic: retrospective. Not predictive of benefit from PD-1 blockade. Investigational	[20,49]
MHC class II (HLA-DR IHC; *CIITA* alteration by FISH/sequencing)	Not assessed	Retained HRS-cell MHC class II associated with complete remission after nivolumab	Predictive for PD-1 blockade: exploratory. Prognostic after chemotherapy: heterogeneous across studies. Investigational	[19,20,49,50]
CD68/CD163 (macrophages)	Not part of standard panel	Quantitative/spatial macrophage density and polarization	Prognostic: inconsistent thresholds across cohorts. Investigational	[48,51–54]
CTLA-4, LAG-3, TIM-3, TIGIT	Not assessed	Extended checkpoint panel; rationale for combination immunotherapy	Investigational	[37,55,56]
FOXP3 (Treg)/ Granzyme B (cytotoxic)	Not assessed	Treg: cytotoxic-cell ratio	Prognostic: single retrospective series. Investigational	[57]

Routine, established routine diagnostic biomarker; investigational, research use only. Prognostic, associated with outcome irrespective of therapy; predictive, associated with benefit from a specific therapy. No marker listed is currently required to establish eligibility for PD-1 blockade or brentuximab vedotin. Abbreviations: EBER, Epstein–Barr virus-encoded small RNA; IHC, immunohistochemistry; PFS, progression-free survival.

3. Immune Profiling: Checkpoints, Antigen Presentation, and Immune Escape

The cHL microenvironment is now understood as an actively engineered, immune-privileged niche rather than an incidental bystander population [58,59]. HRS cells secrete cytokines and chemokines that recruit a specific immune infiltrate—including CD4+ T cells that physically rosette around HRS cells, regulatory T cells (Tregs), M2-polarized tumor-associated macrophages (TAMs), eosinophils, and mast cells—while simultaneously deploying multiple, partially redundant mechanisms of immune evasion [51,57,60]. The predominance of CD4+ T cells is not incidental but actively orchestrated by HRS cells:

HRS cells produce the chemokines CCL17/TARC and CCL22/MDC, which attract CCR4-expressing Th2 and regulatory CD4+ T cells [61]; rosetting CD4+ T cells are retained in close contact with HRS cells through immunological synapses involving HLA class II and CD58 [60]; HRS-cell-derived galectin-1 favors a Th2/regulatory T-cell-skewed infiltrate and the selective apoptosis of Th1 and cytotoxic effector cells [62]; and frequent loss of MHC class I on HRS cells limits the stimulus for CD8+ T-cell expansion [20,22]. As a consequence, CD8+ T cells are relatively scarce in the immediate vicinity of HRS cells [30,31]. The composition of this recruited infiltrate is not static: a small retrospective series has suggested that it differs between patients who respond to frontline ABVD and those who do not [63,64], and larger correlative studies, including one embedded in the E2496 Intergroup trial, have shown that its composition is associated with outcome [51,52]. These data support the prognostic relevance of the immune ecosystem, whereas its predictive value for specific therapies remains to be established prospectively.

The best-characterized evasion mechanism is overexpression of PD-L1 and PD-L2, driven by 9p24.1 copy-number alterations, which are detectable in nearly all cases (97% in the largest FISH series), most frequently as relative copy gain (56%) and as amplification in about one-third of cases (36%), and further enhanced transcriptionally through JAK2-mediated signaling [17,18]. The level of 9p24.1 alteration itself stratifies outcome after standard therapy, amplification being associated with shorter progression-free survival [18]; broader profiling of checkpoint-protein expression across the T-cell and macrophage compartments has further suggested, in a retrospective cohort, that the balance of inhibitory and stimulatory signals is more strongly associated with outcome than any single marker [65].

In the setting of PD-1 blockade, the most informative tissue data derive from the correlative analysis of the CheckMate 205 trial. In patients with relapsed/refractory cHL treated with nivolumab, higher-level 9p24.1 copy gain and higher PD-L1 expression on HRS cells were associated with longer progression-free survival, and HRS-cell expression of MHC class II was associated with complete remission, whereas β2M/MHC class I expression was not predictive of complete remission or progression-free survival [49]. Peripheral blood and single-cell studies point in the same direction: response to PD-1 blockade has been associated with the abundance and T-cell receptor diversity of circulating CD4+ T cells and with B-cell features; PD-1 is expressed in cHL not only by T cells but also by NK cells and monocytes/macrophages; and a proinflammatory IL1β+ monocyte/macrophage signature has been linked to resistance [66–68]. Together, these findings indicate that the efficacy of PD-1 blockade in cHL relies largely on MHC class II-restricted CD4+ T-cell responses and on MHC class I-independent innate effectors rather than on classical CD8+ cytotoxicity. They also mean that MHC class I and class II loss cannot be regarded as interchangeable escape mechanisms: their clinical meaning differs between chemotherapy-era prognosis and response to PD-1 blockade. Importantly, however, these associations derive from retrospective analyses of relatively small trial subsets; no validated cut-off has been defined for PD-L1 expression, 9p24.1 copy number, or MHC class II expression, and responses are also observed in patients with lower PD-L1 expression. None of these parameters is therefore currently used to select or exclude patients for PD-1 blockade [40,49,69].

Distinguishing a predictive from a prognostic effect is not straightforward with the data currently available. A biomarker is prognostic if it is associated with outcome irrespective of the treatment received, and predictive only if its association with outcome differs according to treatment; formally, a predictive effect requires a significant treatment-by-biomarker interaction, tested prospectively or in a prospective–retrospective analysis of archived specimens from a randomized trial comparing the therapy of interest with a control [70,71]. CheckMate 205 and KEYNOTE-087 were single-arm studies, so that associations observed within them cannot, on their own, separate a predictive effect of PD-1

blockade from a general prognostic effect in relapsed/refractory disease [49,72,73]. Indirect support for a therapy-specific effect comes from the observation that some of these biomarkers behave differently after chemotherapy and after PD-1 blockade: 9p24.1 amplification was associated with shorter progression-free survival after standard first-line therapy [18], whereas higher-level 9p24.1 copy gain was associated with longer progression-free survival after nivolumab [49]; decreased or absent β2M/MHC class I expression was associated with inferior progression-free survival after first-line chemotherapy with or without radiotherapy [20] but not with outcome after nivolumab [49]; and decreased or absent MHC class II expression was unrelated to outcome after first-line therapy in the same series [20] but was associated with a lower complete remission rate after nivolumab [49]. Such therapy-dependent differences are consistent with, but do not prove, a predictive effect, because the cohorts differ in disease setting (newly diagnosed versus relapsed after ASCT), endpoints, and scoring methods. To our knowledge, no treatment-by-biomarker interaction analysis of these tissue biomarkers has been reported from a randomized trial of PD-1 blockade in cHL, such as KEYNOTE-204 (pembrolizumab versus brentuximab vedotin) [74] or SWOG S1826 (nivolumab-AVD versus brentuximab vedotin-AVD) [75]; such analyses represent the most direct route to establishing predictive value. In the first trial of nivolumab in cHL, all evaluable pretreatment specimens showed 9p24.1 copy gain and increased PD-L1/PD-L2 expression [76], and because 9p24.1 alterations are near-universal, a biomarker-negative population large enough to test whether therapy could safely be withheld would be very small.

Antigen presentation is concurrently disrupted at both MHC class I and class II. Loss of beta-2-microglobulin (B2M), through mutation or deletion, abrogates surface MHC class I expression and was associated with inferior outcome after standard chemotherapy, independently of 9p24.1 status, in a retrospective series [20], but, as noted above, does not predict failure of PD-1 blockade [49]. CIITA gene fusions, first described as a recurrent structural variant in cHL and primary mediastinal large B-cell lymphoma, transcriptionally silence MHC class II while simultaneously juxtaposing CIITA to strong enhancers that drive overexpression of its fusion partners—a dual mechanism combining immune escape with oncogenic dysregulation [19]. The prognostic significance of MHC class II loss after conventional chemotherapy, by contrast, has been heterogeneous across studies, with an adverse impact reported in some series but not in others [20,50]. These lesions are not mutually exclusive. In a series of 108 uniformly treated patients, decreased or absent β2M/MHC class I and MHC class II expression on HRS cells was found in 79% and 67% of cases, respectively, with no significant association between the two [20]; given the near-universal 9p24.1 alterations described above, most tumors combine 9p24.1-driven PD-L1/PD-L2 overexpression with reduced expression of at least one class of MHC molecules. Whole-exome sequencing of flow-sorted HRS cells has likewise identified recurrent alterations in several immune-evasion pathways—including 9p/9p24.1 copy gains and genes of the MHC class I antigen-presentation pathway such as B2M, the latter more frequent in EBV-negative cases—supporting complementary rather than mutually exclusive mechanisms of immune evasion [22,23]; CIITA fusions, by contrast, account for only a minority of cases with MHC class II loss [19,20]. Whether the combination of these alterations carries prognostic or predictive information beyond that of each alteration alone has been examined only to a limited extent. In the chemotherapy-treated series, 9p24.1 amplification was associated with inferior progression-free survival in patients whose HRS cells had decreased or absent β2M/MHC class I expression, whereas no effect was apparent in the few patients (n = 3) with amplification and retained MHC class I expression; in multivariable models, decreased MHC class I expression retained adverse prognostic significance independently of 9p24.1 amplification and advanced stage [20]. In the setting of PD-1 blockade, the combined effect

of these alterations has not, to our knowledge, been formally evaluated, and no composite score has been validated [49]. The coexistence of these lesions should therefore be regarded as biologically established, whereas its clinical significance remains investigational.

Beyond the PD-1 axis, additional checkpoint molecules shape the cHL microenvironment. CTLA-4 has been identified on a distinct, largely PD-1-negative T-cell subset within the HRS-cell niche, suggesting parallel, non-overlapping inhibitory circuits that could inform rational combination checkpoint strategies rather than sequential single-agent blockade [55]. LAG-3, TIM-3, and TIGIT, together with other emerging checkpoint targets, have also been reported on subsets of T cells within the cHL microenvironment, broadening the immune-checkpoint landscape and the corresponding therapeutic opportunity beyond PD-1/PD-L1 alone [37,56].

Macrophages represent a second, largely independent, prognostic arm of the immune microenvironment. Since the original description linking high densities of CD68-positive macrophages to inferior survival, subsequent studies using CD163 and combinations of CD68 clones have shown that macrophage polarization state and spatial distribution—rather than raw density alone—carry prognostic information, and that their prognostic impact in chemotherapy-treated patients depends on the expression of checkpoint molecules, such as PD-L1 and IDO-1, by the macrophages themselves [48,51–54]. That the same nominal biomarker (a CD68- or CD163-defined macrophage count) has yielded inconsistent prognostic thresholds across cohorts is itself instructive: it illustrates why a single immunohistochemical marker, however biologically plausible, cannot substitute for a multiparametric, spatially resolved assessment of the myeloid compartment. EBV-positive cases show a distinct macrophage and cytokine profile, and LMP1 expression has been linked to outcome in some series [43]; however, the prognostic value of EBV status has varied across studies, age groups, and regions, and a meta-analysis of 42 studies found an association of EBV positivity with poorer overall survival, with substantial heterogeneity across subgroups. These observations further illustrate how viral status intersects with the broader immune landscape [43,44]. Collectively, these findings establish immune profiling—encompassing checkpoint expression, antigen-presentation machinery, and macrophage/T-cell composition—as a biologically indispensable, but conventionally invisible, layer of cHL pathology, while also showing that most immune-profiling biomarkers remain prognostic associations derived from retrospective cohorts rather than validated predictive tools.

These convergent mechanisms of immune evasion—checkpoint overexpression, antigen-presentation loss, and T-cell dysfunction—are not randomly distributed within the tumor but are organized in a spatially structured niche immediately surrounding the HRS cell, in which the physical proximity of immune effectors to the malignant clone shapes the local balance between immune surveillance and immune privilege (Figure 2).

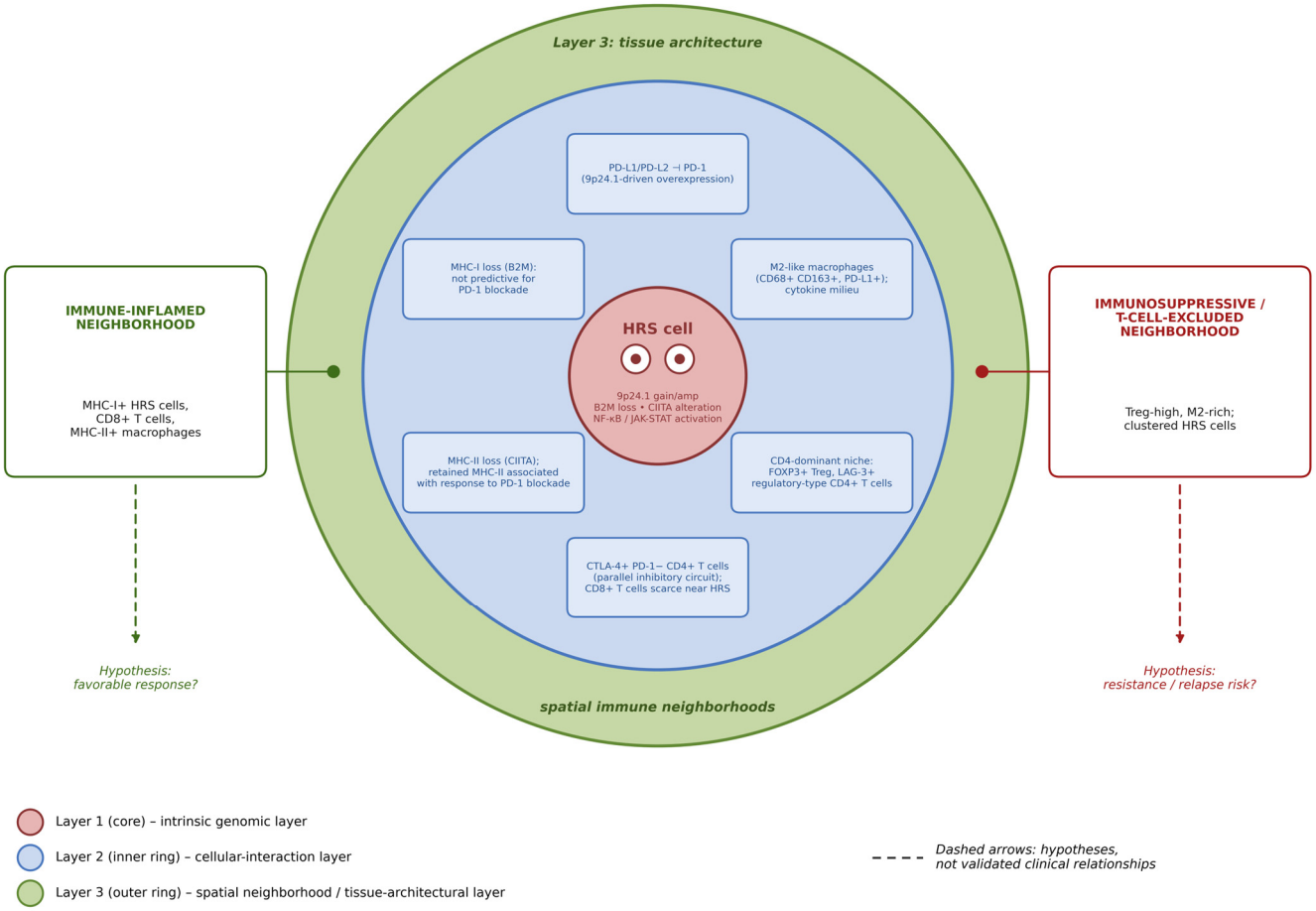


Figure 2. Layered conceptual model of immune evasion around the Hodgkin and Reed–Sternberg (HRS) cell. Layer 1 (core): intrinsic genomic alterations—9p24.1 copy gain/amplification [17,18], B2M loss [20,22], CIITA alterations [19], and NF-κB/JAK-STAT activation [4,21–23]. Layer 2 (inner ring): cellular interactions—PD-L1/PD-L2–PD-1 engagement [17,18]; M2-like, PD-L1+ macrophages [48,51–54]; a CD4-dominant T-cell niche that includes FOXP3+ regulatory T cells and LAG-3+ regulatory-type CD4+ T cells [30,31,57]; CTLA-4+ PD-1− CD4+ T cells [55]; and MHC class I and class II loss, shown separately because retained MHC class II has been associated with response to PD-1 blockade, whereas MHC class I status has not [49]. CD8+ T cells are relatively scarce in the immediate vicinity of HRS cells [30,31]. Layer 3 (outer ring): tissue-architectural layer contrasting immune-inflamed neighborhoods (MHC class I+ HRS cells with CD8+ T cells and MHC class II+ macrophages) and immunosuppressive, regulatory T-cell-high or T-cell-excluded neighborhoods, as described in newly diagnosed cHL [1]. Dashed arrows linking these neighborhood types to treatment response or to resistance/relapse risk represent hypotheses, not validated clinical relationships or decision rules; the study that introduced these neighborhood categories did not assess outcome [1]. Figure 2 depicts the layered conceptual model (genomic, cellular, and architectural layers), whereas Figure 3 depicts the cellular composition of the HRS-cell niche.

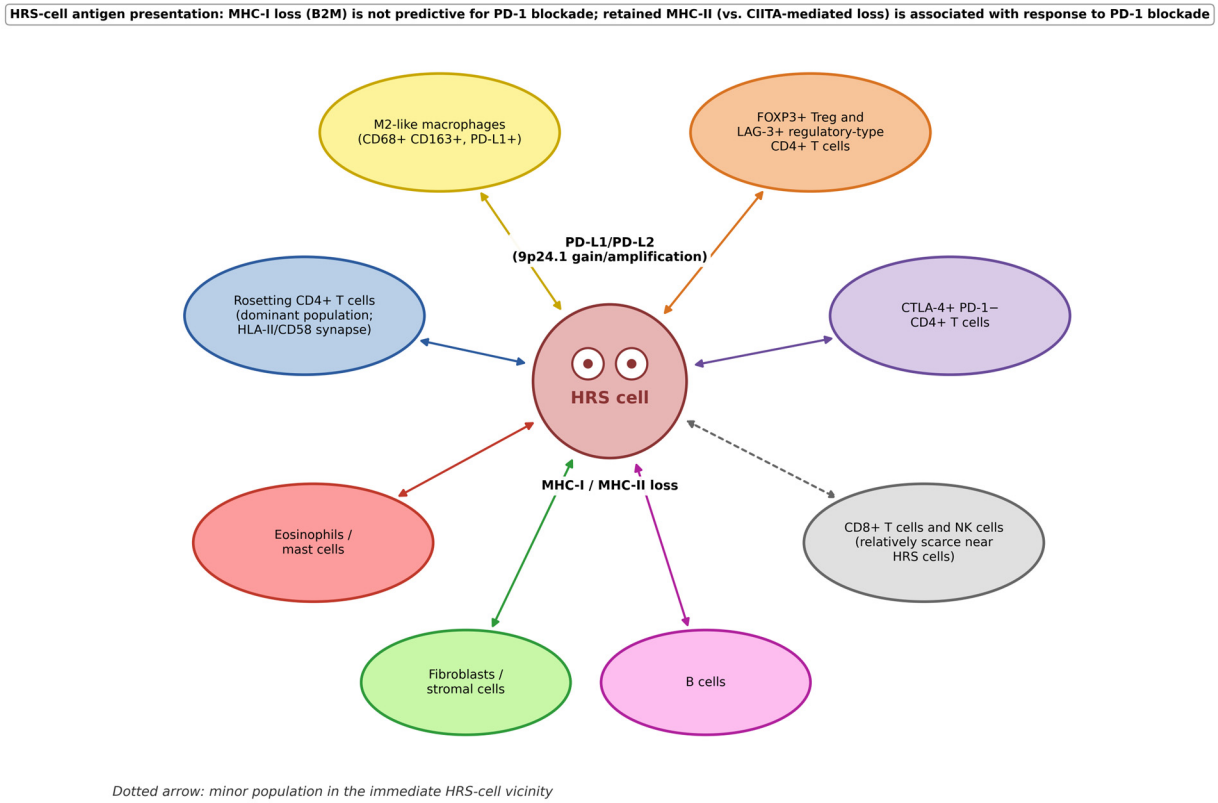


Figure 3. Cellular composition of the Hodgkin and Reed–Sternberg (HRS) cell niche. The niche is dominated by CD4+ T cells, including rosetting CD4+ T cells held in contact with HRS cells through HLA class II- and CD58-dependent immunological synapses [60], FOXP3+ regulatory T cells [57], LAG-3+ regulatory-type CD4+ T cells [30,31], and CTLA-4+ PD-1− CD4+ T cells [55]. Other components include M2-like CD68+ CD163+ macrophages, which frequently express PD-L1 [48,51–54]; B cells, eosinophils, mast cells, and fibroblasts/stromal cells [3,58,59]; and CD8+ T cells and NK cells, which are relatively scarce in the immediate vicinity of HRS cells (dotted arrow) but may contribute, together with CD4+ T cells, to the effect of PD-1 blockade [30,31,66,67]. Central labels indicate the main HRS-cell-intrinsic escape mechanisms: 9p24.1-driven PD-L1/PD-L2 overexpression [17,18], MHC class I loss (B2M) [20], and MHC class II loss (CIITA) [19]; retained MHC class II, unlike MHC class I, has been associated with response to PD-1 blockade [49]. Arrows denote bidirectional signaling, including checkpoint ligand–receptor interactions and cytokine/chemokine crosstalk (e.g., CCL17/TARC and CCL22 attracting CCR4+ CD4+ T cells [61]). Unlike Figure 2, which presents a layered conceptual model, this figure is intended as a cellular inventory of the niche.

4. Spatial Immunopathology: Multiplex, Imaging Mass Cytometry, and Digital Spatial Profiling

Because immune escape in cHL depends on direct, juxtacrine interactions between rare HRS cells and their immediate neighbors, bulk or single-marker assays cannot fully capture the spatial logic of the tumor-immune synapse; the technologies summarized in Table 3 were developed to close precisely this gap. Multiplex immunohistochemistry and immunofluorescence (mIHC/mIF) allow simultaneous visualization of multiple markers—typically six to nine with commercially available tyramide-based multiplex immunofluorescence—on a single tissue section while preserving spatial context. We have previously proposed that mIHC-based characterization of the cells directly surrounding HRS cells, rather than average tissue-wide marker positivity, could help optimize checkpoint-inhibitor therapy in relapsed or progressive cHL [24]; this remains a proposal that has not yet been tested in a prospective patient-selection study. Highly multiplexed imaging extends this principle to dozens of parameters, either through cyclic immunofluo-

rescence (e.g., Cell DIVE and CODEX/PhenoCycler) or through metal-tagged antibodies (imaging mass cytometry, IMC). Using cyclic immunofluorescence and spatial transcriptomics in 36 newly diagnosed cHL, Pourmaleki et al. linked MHC class I expression on HRS cells to immune-inflamed neighborhoods containing CD8+ T cells and MHC class II+ macrophages, and identified T-cell-excluded and regulatory T-cell-high neighborhoods; this study did not include an outcome endpoint [1]. Using IMC on 71 paired diagnostic and relapse biopsies from patients with relapsed/refractory cHL, Aoki et al. developed a four-parameter spatial score (RHL4S: CXCR5+ HRS cells, PD-1+ CD4+ T cells, CD68+ macrophages, and CXCR5+ B cells) that separated patients with different outcomes after high-dose chemotherapy and autologous stem-cell transplantation (ASCT) and was validated in an independent cohort using multicolor immunofluorescence [25]. Notably, this score is associated with post-transplant outcome, not with response to checkpoint blockade, and has not been evaluated prospectively. Antecedent mass cytometry (CyTOF) and single-cell RNA-sequencing studies of dissociated cHL tissue had already shown that the T-cell compartment is dominated by a CD4-rich, regulatory and exhausted phenotype distinct from that of reactive lymph nodes, providing the immunophenotypic foundation that spatial platforms have since mapped back onto intact tissue architecture [30,31].

Digital spatial profiling (DSP) platforms couple region-of-interest selection with multiplexed protein or RNA readout, enabling quantitative, spatially resolved analysis of standard formalin-fixed, paraffin-embedded tissue without the need for tissue dissociation [26]. Applied specifically to cHL, DSP has been used to dissect the spatial dynamics of CD4+ T-cell subsets around HRS cells [27], and genome-scale spatial mapping approaches have begun to identify tumor-cell survival factors embedded within the local microenvironment that would remain invisible to bulk sequencing of whole tissue sections [2]. Spatial transcriptomics, which overlays whole-transcriptome or targeted gene-expression data onto tissue coordinates, is rapidly being adopted across lymphoma pathology generally and is beginning to generate cHL-specific insights into the spatial organization of the HRS-cell niche and its surrounding stroma [28,29]. Single-cell RNA sequencing has complemented these spatial approaches by defining disease-specific T-cell subsets that are not found in reactive lymphoid tissue, several of which appear to represent direct products of chronic antigen exposure and checkpoint engagement within the tumor niche [31,77]. More recently, single-cell RNA sequencing combined with spatial analysis of patients treated with PD-1 blockade has identified complementary roles of CD4+ T cells, B cells, and IL1β+ monocytes/macrophages in response and resistance [68], and genome-scale spatial mapping has shown that the HRS-cell neighborhood forms a distinct niche enriched in helper T cells [2].

These studies, however, should be interpreted as biological discovery or retrospective validation rather than clinically validated prediction. Most derive from single institutions or relatively small cohorts (typically a few dozen to around one hundred patients), analyzed on specialized platforms with bespoke marker panels and analytical pipelines; reproducibility across platforms, laboratories, and pre-analytical conditions has not been systematically assessed; and, to our knowledge, no spatial signature has yet been validated prospectively or incorporated into treatment decisions in cHL. Accordingly, the terms "predict" and "predictor" in this context refer to statistical associations with outcome in discovery or retrospective validation cohorts, and all spatial technologies are classified as investigational in Tables 3 and 6.

Collectively, these technologies convert the tumor microenvironment from a qualitative background observation into a quantitative, spatially resolved biomarker source, and suggest that where immune cells sit relative to HRS cells may be as biologically—and potentially clinically—informative as which immune cells are present in the first place (Figure 3).

Table 3. Spatial, single-cell, and computational technologies applied to the classic Hodgkin lymphoma tumor microenvironment, with current level of clinical implementation.

Technology	Representative Platforms	Readout	Application in cHL (Study Design)	Current Implementation Level	Ref.
Spatial and Single-Cell Technologies					
Multiplex IHC/ immunofluorescence (mIHC/mIF)	Opal (tyramide signal amplification); sequential chromogenic mIHC	Typically 6–9 protein markers per section	Immune composition around HRS cells; proposed for optimizing checkpoint-inhibitor therapy (perspective); prognostic checkpoint profiling (retrospective)	Investigational (feasible on FFPE; not standardized)	[24,54,65]
Cyclic immunofluorescence	Cell DIVE; CODEX/PhenoCycler	Tens of protein markers, single-cell spatial resolution	HRS-cell neighborhood mapping in newly diagnosed cHL (no outcome endpoint)	Investigational	[1]
Imaging mass cytometry (IMC)	Hyperion	~40 metal-tagged markers, subcellular resolution	Spatial score (RHL4S) associated with outcome after ASCT in R/R cHL (retrospective; independent validation by mIF)	Investigational	[25]
Mass cytometry (CyTOF, non-spatial)	Helios	High-dimensional single-cell immunophenotyping of dissociated tissue or blood	T-cell subset discovery; peripheral immune signature associated with response to PD-1 blockade	Investigational	[30,66]
Digital spatial profiling (DSP)	NanoString GeoMx	Region-of-interest protein/RNA quantification on FFPE tissue	CD4+ T-cell spatial dynamics	Investigational	[26,27]
Spatial transcriptomics	Visium; Slide-seqV2; CosMx SMI	Whole/targeted transcriptome with spatial coordinates	HRS-cell niche organization; tumor-cell survival factors	Investigational	[2,28,29]
Single-cell RNA sequencing	Droplet-based scRNA-seq platforms	Transcriptome-wide, single-cell resolution	Disease-defining T-cell subsets; immune rewiring associated with resistance to PD-1 blockade	Investigational	[31,68,77]
Digital pathology and computational tools (not multi-omic technologies)					
Whole-slide imaging/ digital pathology	Slide scanner + digital viewer	Digitized H&E/ IHC slides	Remote consultation; diagnostic concordance review	Routine in some centers (consultation; primary diagnosis where validated)	[32]
Digital image analysis	Quantitative image-analysis software	Automated cell quantification on WSI	HRS-cell and T-cell content associated with outcome after ABVD (two-center, retrospective; no external validation)	Investigational	[78]
Machine-learning/ deep-learning models	Convolutional neural-network classifiers	Automated classification/ quantification	cHL: deep-learning quantification of picrosirius red-stained collagen in pediatric HL (not sufficient as stand-alone prognostic tool). Other lymphomas: subtype classification (retrospective proof of concept)	Investigational; no cHL-specific tool approved	[33–35,39,79,80]

Abbreviations: ABVD, doxorubicin, bleomycin, vinblastine, dacarbazine; ASCT, autologous stem-cell transplantation; FFPE, formalin-fixed, paraffin-embedded; R/R, relapsed/refractory; WSI, whole-slide imaging. Multiplexing capacity is indicative and depends on platform and panel design.

5. Molecular Pathology: Genomic Landscape and Liquid Biopsy

Because HRS cells constitute such a small fraction of the tumor mass, molecular characterization of cHL required methodological innovation before it could proceed at all. Flow-sorting or laser-capture microdissection of HRS cells followed by exome or genome-wide

sequencing confirmed recurrent alterations converging on the NF-κB pathway, including TNFAIP3/A20 inactivation, alongside the 9p24.1, B2M, and CIITA alterations described above [22,23,81]. Additional recurrent alterations include inactivating mutations of *SOCS1* and *PTPN1* and mutations of *STAT6* and *CSF2RB* (JAK/STAT pathway), *NFKBIE* and *TNFAIP3* mutations and *REL*/2p16 gains (NF-κB pathway), and mutations of *GNA13*, *ITPKB*, *XPO1* (including the E571K hotspot), and *ARID1A* [22,23,81–84]. Contrary to the earlier assumption of a low mutational load, EBV-negative cHL has been shown to carry one of the highest mutational burdens reported across cancers, with microsatellite instability-associated and APOBEC-related signatures—features that may contribute to the efficacy of PD-1 blockade [22]. NF-κB activation, achieved through both canonical and non-canonical routes, appears to be a near-universal feature of HRS cells and cooperates with JAK/STAT signaling to sustain the anti-apoptotic, proliferative, and immunomodulatory phenotype that defines the malignant clone (Table 4) [4,21].

The practical difficulty of obtaining sufficient malignant material from cHL tissue has made circulating tumor DNA (ctDNA) genotyping particularly valuable in this disease. Targeted sequencing of cell-free DNA can recover the mutational profile of HRS cells non-invasively—plasma variant allele fractions often exceed those measured in bulk tissue [85]—and has been used to track clonal evolution and to detect genetic heterogeneity not always appreciated on a single tissue biopsy [82]. Pretreatment and on-treatment ctDNA levels correlate with response and outcome in retrospective and prospective cohorts [82,85,86], and ultrasensitive methods can detect radiographically occult minimal residual disease [85]; however, systematic data on the lead time between molecular and clinical or radiologic relapse remain limited. The approach has been extended to pediatric cHL, in which diagnostic tissue is often especially limited [87], and has been used to define molecularly distinct genomic subtypes directly from plasma—two subtypes (H1 and H2) with distinct clinical, prognostic, transcriptional, and immunological correlates in one study [85], and three biologically defined subtypes, validated in pediatric and adult trial cohorts including HD21, in another [88]. Importantly, these plasma-based classifications were derived in patients whose diagnosis had already been established histologically on tissue; they represent molecular characterization that complements, rather than replaces, the diagnostic biopsy, which remains indispensable to establish the diagnosis, determine the histological subtype, and exclude morphologic and immunophenotypic mimics. Trial-embedded data are now emerging: in a correlative analysis of the S1826 trial, so far reported only in abstract form, ctDNA-based molecular tumor burden after two cycles and at the end of therapy was more strongly associated with outcome than PET-based response assessment [89].

Several limitations nevertheless temper these promising results. Assays differ substantially in technology (hybrid-capture panels, phased-variant enrichment sequencing, digital PCR), gene content, and limits of detection; optimal sampling time-points and thresholds defining molecular response or minimal residual disease have not been harmonized; and, most importantly, no study has yet shown that ctDNA-directed modification of therapy improves patient outcome. The terms “feasible”, “prognostic”, and “clinically actionable” should therefore not be used interchangeably: ctDNA genotyping is feasible and prognostic, but not yet clinically actionable outside clinical trials. At present, therefore, ctDNA has no established clinical utility in cHL for diagnosis, staging, or treatment selection; its use is limited to clinical trials and prospective studies, and it cannot independently guide treatment decisions. Likewise, FISH-based assessment of 9p24.1 and targeted sequencing are technically feasible in specialized laboratories, but because nearly all cases carry a 9p24.1 alteration and no threshold has been validated to withhold therapy, their use to select patients for PD-1 blockade remains investigational. The most realistic near-term

application is ctDNA-based response assessment within prospective trials, where it may complement, and eventually refine, PET-based response adaptation.

The WHO classification has evolved in step with this molecular understanding: the 2016 revision already incorporated emerging genetic insights into lymphoid neoplasm classification generally [8], and both the current fifth edition of the WHO classification [9] and the ICC [10] integrate genetic data into the definition of many lymphoid neoplasms. For cHL, however, the definition and subtyping remain essentially morphologic and immunophenotypic, and no genomic feature is currently required for diagnosis. Molecular pathology in cHL has thus moved from a purely research tool toward a source of biologically informative, and increasingly non-invasively obtainable, biomarkers whose clinical actionability still requires prospective demonstration.

Table 4. Recurrent molecular and genomic alterations in classic Hodgkin lymphoma, distinguishing biologically established alterations from biomarkers used in routine clinical decision-making.

Gene/Locus	Alteration (Approximate Frequency)	Functional Consequence	Biological/ Clinical Significance	Current Clinical Use	Ref.
9p24.1 (*CD274*/ *PDCD1LG2*/*JAK2*)	Copy-number alteration in ~97%: relative copy gain (~56%), amplification (~36%), polysomy (~5%)	Increased PD-L1/PD-L2 transcription; further JAK2-mediated induction	Rationale for PD-1 blockade; amplification associated with shorter PFS after standard therapy; higher-level gain associated with longer PFS after nivolumab	Biologically established; FISH available but not used for treatment decisions (investigational as predictor)	[17,18,49]
B2M	Inactivating mutation/deletion	Loss of surface MHC class I expression	Inferior outcome after chemotherapy (retrospective); not predictive for PD-1 blockade	Biologically established; not used clinically	[20,22,49]
CIITA	Recurrent gene fusion/structural alteration	Loss of MHC class II expression; fusion-partner overexpression	Dual immune-escape/ oncogenic mechanism; retained MHC class II associated with response to PD-1 blockade	Biologically established; not used clinically	[19,49]
NF-κB pathway	*TNFAIP3*/A20 and *NFKBIE* inactivating mutations; *REL*/2p16 gain	Constitutive canonical/ non-canonical NF-κB activation	Supports HRS-cell survival and proliferation	Biologically established; not used clinically	[4,21–23]
JAK/STAT pathway	*SOCS1* and *PTPN1* inactivation; *STAT6* mutation (~30–40%); *CSF2RB* mutation; *JAK2* gain	Constitutive STAT signalling	Cooperates with NF-κB; supports PD-L1 induction	Biologically established; not used clinically	[17,21,22,82,83]
Other recurrently mutated genes	*GNA13*, *ITPKB*, *XPO1* (E571K), *ARID1A*	G-protein, B-cell receptor/calcium, nuclear-export, and chromatin-remodeling pathways	*XPO1* E571K detectable in plasma, with possible prognostic value	Investigational	[22,23,83,84]
IL4R	Truncating mutations	IL-13-dependent signaling	Potential target of IL-4Rα-blocking antibodies (preclinical)	Investigational	[85]
ctDNA-defined genomic subtypes	H1/H2 subtypes; biologically defined ctDNA subtypes	Distinct genomic, transcriptional, and immune profiles	Distinct clinical and prognostic correlates	Investigational	[85,88]
Genome-wide somatic variants (ctDNA)	Variants recoverable from cell-free DNA	Non-invasive genotyping of HRS-cell clone	Disease monitoring, molecular response, and residual-disease detection; prognostic	Investigational; trial-embedded validation ongoing	[82,85–87,89]

Frequencies are approximate and derived from the cited series; they vary with detection method (FISH, tissue sequencing, or ctDNA). Abbreviations: ctDNA, circulating tumor DNA; FISH, fluorescence in situ hybridization; PFS, progression-free survival.

6. Digital Pathology and Artificial Intelligence

The multiplicity of markers, platforms, and spatial layers generated by precision immunopathology creates a practical challenge: reproducible quantification and integration at a scale compatible with routine diagnostic workflows. Whole-slide imaging (WSI) converts glass slides into high-resolution digital files that can be annotated, quantified, and shared for remote consultation; studies directly comparing digital and glass-slide diagnosis in hematopathology have identified specific, recurring discrepancy patterns that now inform quality-assurance protocols for digital adoption in routine practice [32]. Once digitized, tissue sections become amenable to computational analysis: in other lymphoma entities, retrospective proof-of-concept studies have shown that deep-learning classifiers trained on whole-slide images can, for example, distinguish follicular lymphoma from follicular hyperplasia [33] or classify chronic lymphocytic leukemia and follicular lymphoma images [80] with high accuracy. Evidence specific to cHL is considerably more limited. Whole-slide digital image analysis has been used to quantify HRS-cell and T-cell content as predictors of outcome after ABVD in a two-center retrospective cohort of 85 patients, without external validation [78], and a deep-learning approach has been applied to quantify picrosirius red-stained collagen as a candidate prognostic metric in pediatric Hodgkin lymphoma, the authors concluding that it was not sufficiently accurate to serve as a stand-alone prognostic tool [79].

Beyond diagnostic classification, machine-learning approaches are being developed across the full spectrum of lymphoma histopathology—from initial diagnosis and subtyping to prognostic modeling and treatment-response prediction—with a rapidly growing literature that includes systematic reviews [34] spanning conventional machine learning, deep convolutional networks, and, increasingly, multimodal models that combine histology with clinical and molecular data. More broadly, artificial intelligence in digital pathology has been framed as a foundational enabling technology for precision oncology generally, capable of extracting quantitative, reproducible features from routine histology that complement, and in some cases anticipate, molecular and genomic findings [35]. A dedicated synthesis has similarly outlined how artificial intelligence may help resolve specific diagnostic and prognostic challenges in cHL, from subtype recognition to biomarker quantification [39]. In cHL specifically, where HRS cells are rare and manual immune-cell quantification is labor-intensive and subject to substantial inter-observer variability, algorithmic quantification of checkpoint expression, macrophage density, and spatial neighborhood composition could offer a route to standardized, scalable biomarker assessment that would be impractical to achieve by manual review alone (Table 3).

Realizing this potential in routine practice will require several concurrent developments: prospective, multi-institutional validation of candidate algorithms on cohorts that reflect real-world staining and scanning variability rather than single-center training data; standardization of pre-analytical variables, including fixation time, antibody clone, and antigen-retrieval protocol, all of which materially affect quantitative immunohistochemical output; transparent reporting of model performance across patient subgroups to avoid propagating existing diagnostic biases into automated tools; and regulatory frameworks for clinical deployment of computational pathology algorithms that remain, in most jurisdictions, under active development rather than fully established. These requirements are particularly pressing in cHL. To our knowledge, no AI tool has been approved by regulatory agencies or deployed in clinical practice for cHL-specific diagnostic, prognostic, or predictive use; most published models are retrospective proofs of concept derived from one or a few institutions, and their performance is vulnerable to dataset shift—including scanner and staining variability, differences in case mix and histological subtype distribution, and changes in pre-analytical handling. Interpretability of model outputs, external

validation on independent multi-institutional cohorts, and prospective evaluation of the impact on diagnostic accuracy and patient outcome are therefore prerequisites for clinical use [34,35,39]. Accordingly, all AI-based applications are classified as investigational in Tables 3 and 6.

7. Clinical Translation: Biomarker-Driven Immunotherapy

The molecular and immune biology described above has already reshaped clinical management of cHL, and is summarized alongside its underlying rationale in Table 5. The demonstration that HRS cells almost universally overexpress PD-L1/PD-L2 provided the rationale for testing PD-1 blockade in relapsed or refractory cHL, and nivolumab produced substantial response rates in an early-phase trial in heavily pretreated patients, a result subsequently confirmed with durable responses in an expanded, multicohort phase II study [72,76]. Pembrolizumab likewise showed marked activity in relapsed or refractory disease [73] and, in a randomized phase III comparison, demonstrated superior progression-free survival compared with brentuximab vedotin, establishing checkpoint blockade as a standard option in this clinical setting [74]. Brentuximab vedotin itself, targeting CD30, produced durable remissions in its pivotal phase II trial in relapsed or refractory disease [90] and, when incorporated into frontline combination chemotherapy, improved outcomes for patients with advanced-stage disease in the ECHELON-1 trial, with benefit sustained on extended follow-up [91,92]. More recently, PD-1 blockade has moved into the frontline setting: in the phase III SWOG S1826 trial, nivolumab plus doxorubicin, vinblastine, and dacarbazine (N-AVD) improved progression-free survival compared with brentuximab vedotin-AVD in patients aged 12 years or older with newly diagnosed stage III–IV cHL [75], with benefit maintained at 3 years in adolescents [93] and particularly pronounced, together with better tolerability, in patients aged 60 years or older [94]. On the basis of S1826, the U.S. Food and Drug Administration (FDA) approved nivolumab in combination with AVD in March 2026 for adult and pediatric patients aged 12 years or older with previously untreated stage III–IV cHL, without any biomarker requirement [95]. In parallel, the PET-guided BrECADD regimen (brentuximab vedotin, etoposide, cyclophosphamide, doxorubicin, dacarbazine, and dexamethasone) proved more effective and better tolerated than escalated BEACOPP in the phase III GHSG HD21 trial [96], establishing a further CD30-directed frontline standard. Regulatory approval, labeled indications, reimbursement, and availability of these frontline regimens nevertheless differ between regions: for example, N-AVD has been approved by the FDA [95] and subsequently by the European Commission [97], whereas BrECADD has been approved in the European Union [98] but not, to our knowledge, in the United States. The choice among these regimens therefore also depends on local regulatory status, reimbursement, and guidelines. Notably, none of these regimens requires a tissue biomarker for patient selection beyond the diagnosis of cHL itself. Response-adapted strategies using interim PET-CT imaging to escalate or de-escalate chemotherapy intensity, validated in large international trials, further illustrate how an imaging-based biomarker already personalizes treatment in this disease, providing a template that molecular and immune biomarkers may eventually extend or refine [15,16].

Despite this progress, predictive biomarkers for checkpoint-inhibitor response in cHL remain less mature than in many solid tumors, where tumor mutational burden and PD-L1 immunohistochemistry are more directly actionable; lymphoma biology, with its distinct genetic mechanism of PD-L1 upregulation and its reliance on innate as well as adaptive antitumor immunity, requires dedicated predictive frameworks rather than direct extrapolation from solid-tumor paradigms [69]. In particular, no percentage of PD-L1-, PD-1-, or CD30-positive cells has been validated as a threshold predicting efficacy. CD30 is expressed by HRS cells by definition, and the brentuximab vedotin trials required only a diagnosis

of CD30-positive cHL [90,91]; PD-L1 is expressed by HRS cells in the large majority of cases, PD-1 is expressed by T cells and other immune effectors in the microenvironment rather than by HRS cells, and the checkpoint-inhibitor trials did not require any threshold of PD-L1 or PD-1 expression [72–74,76]. Retrospective correlative analyses have associated higher PD-L1 expression and higher-level 9p24.1 gain with longer progression-free survival after nivolumab, but responses also occur in patients with lower expression [49]. The precision immunopathology approach outlined in this review—integrating 9p24.1 status, antigen-presentation competence, spatial immune topology, and computational quantification—represents a candidate framework for developing and prospectively testing such biomarkers [5,6,99]. With the move of PD-1 blockade into first-line therapy, the clinically relevant questions have changed: rather than selecting patients for checkpoint blockade at relapse, biomarkers will be needed at diagnosis to identify patients likely to be cured with N-AVD who might be candidates for de-escalation, patients at risk of primary resistance who might benefit from alternative or intensified strategies, and patients in whom ctDNA-based response assessment could complement PET [89]. In practical terms, any biomarker intended to guide frontline PD-1 blockade would have to be assessed on the diagnostic biopsy, before the first treatment cycle and with a turnaround time compatible with prompt initiation of therapy, and its value would have to be demonstrated as a treatment-by-biomarker interaction in randomized comparisons of PD-1-based and CD30-directed frontline regimens, for example through prospective–retrospective analyses of specimens banked within such trials [71,75]. Until such data are available, pretreatment assessment of PD-L1, 9p24.1, or MHC class II should neither delay treatment nor determine the choice between N-AVD, brentuximab vedotin-AVD, and BrECADD, and banking of diagnostic tissue and plasma is the most useful contribution that pathology can make today (Tables 7 and 8).

Table 5. Approved and investigational immunotherapeutic strategies in classic Hodgkin lymphoma and tissue biomarker requirements for their use.

Agent/Strategy	Target/Mechanism and Biological Rationale	Setting and Pivotal Evidence	Tissue Biomarker Required for Eligibility	Ref.
Nivolumab	Anti-PD-1 monoclonal antibody; 9p24.1-driven PD-L1/ PD-L2 overexpression	R/R cHL: CheckMate 039 (phase I); CheckMate 205 (phase II)	None	[72,76]
Pembrolizumab	Anti-PD-1 monoclonal antibody; as above	R/R cHL: KEYNOTE-087 (phase II); KEYNOTE-204 (phase III vs. brentuximab vedotin)	None	[73,74]
Nivolumab + AVD (N-AVD)	Anti-PD-1 antibody combined with chemotherapy	Frontline, stage III–IV, age ≥12 years: SWOG S1826 (phase III vs. BV-AVD), including adolescent and ≥60-year analyses; approved by the FDA (March 2026) and the European Commission; regulatory status varies by region	None	[75,93–95,97]
Brentuximab vedotin	Anti-CD30 antibody–drug conjugate (MMAE); CD30 expression on HRS cells	R/R cHL: pivotal phase II; frontline advanced stage: ECHELON-1 (BV-AVD)	None (CD30 expressed by definition)	[90–92]

Table 5. *Cont.*

Agent/Strategy	Target/Mechanism and Biological Rationale	Setting and Pivotal Evidence	Tissue Biomarker Required for Eligibility	Ref.
BrECADD	Anti-CD30 antibody–drug conjugate within intensive chemotherapy	Frontline advanced stage, PET-guided: GHSG HD21 (phase III vs. eBEACOPP); approved in the European Union, regulatory status varies by region	None	[96,98]
Response-adapted chemotherapy	Interim PET-CT-guided escalation/de-escalation; early metabolic response predicts outcome	RATHL; SWOG S0816	Not applicable (imaging biomarker)	[15,16]
Investigational combination strategies	Dual checkpoint blockade; checkpoint inhibitor + CD30-directed ADC; LAG-3-, TIM-3-, or TIGIT-directed agents; targeting parallel, non-overlapping inhibitory circuits	Early-phase clinical trials	None validated; tissue biomarkers explored in correlative studies	[37,55,56,69]

Abbreviations: ADC, antibody–drug conjugate; AVD, doxorubicin, vinblastine, dacarbazine; BV, brentuximab vedotin; eBEACOPP, escalated BEACOPP; MMAE, monomethyl auristatin E; R/R, relapsed/refractory.

8. Towards an Integrated, Ecosystem-Centered Diagnostic Framework

The technologies reviewed here do not operate in isolation but function as complementary layers of a single, increasingly unified diagnostic process (Table 1, Figure 1). Morphology and standard immunohistochemistry remain the indispensable foundation, establishing the diagnosis and histological subtype upon which every subsequent layer depends. Immune and checkpoint profiling adds information about the functional state of the tumor-immune interaction; spatial technologies situate that information within intact tissue architecture; molecular pathology, including ctDNA-based liquid biopsy, provides genetic context and a non-invasive monitoring tool; and digital pathology with artificial intelligence supplies the computational infrastructure required to quantify and integrate these otherwise disparate, high-dimensional data streams reproducibly.

Conceptually, this can be visualized as concentric layers of information radiating outward from the HRS cell itself: an intrinsic genomic layer comprising 9p24.1, B2M, CIITA, and NF-κB/JAK-STAT alterations; an immediate cellular-interaction layer comprising checkpoint ligand–receptor engagement, antigen presentation, and cytokine crosstalk with adjacent T cells and macrophages; and a tissue-architectural layer comprising the spatial organization and topology of the broader immune and stromal infiltrate (Figure 2). A fully integrated diagnostic workflow would capture tissue at biopsy, apply standard morphology and immunohistochemistry for diagnosis, layer on spatial and molecular assays selected according to clinical context—for example, ctDNA for baseline risk assessment and response monitoring, or 9p24.1 FISH and MHC class II immunohistochemistry as candidate predictors of benefit from PD-1 blockade within clinical trials—integrate tissue-derived data with plasma (ctDNA, serum TARC/CCL17) and imaging (baseline MTV, interim PET) biomarkers, and use digital pathology and machine-learning tools to standardize quantification and support clinical decision-making, all feeding into a single, integrated report (Figure 4, Tables 6–8).

Two non-tissue biomarkers are closely linked to cHL immunobiology and already used in clinical research. Serum or plasma TARC/CCL17, secreted by HRS cells to recruit CCR4+ CD4+ T cells into the niche [61], reflects disease activity and has been studied as an early response marker in prospective cohorts [100,101] and in correlative studies embedded in the PET-adapted SWOG S0816 and HD0607 trials, in which higher TARC levels after two cycles or at the end of therapy were associated with inferior progression-free survival, also in patients with a negative interim PET [102,103], although assays and cut-offs have not been harmonized; baseline total MTV on PET-CT captures tumor burden and adds prognostic information to clinical risk factors [14]. Together with ctDNA [82,85,86,88,89], these biomarkers provide a non-invasive, repeatable complement to the single diagnostic biopsy, and they are explicitly included as plasma and imaging inputs in the revised integrated workflow (Figure 4).

To make the framework operational, Table 6 grades each candidate biomarker or assay according to the clinical question addressed, the level of evidence (discovery, retrospective validation, prospective/trial-embedded validation, or guideline-endorsed), feasibility on routine FFPE material, turnaround time, availability of standardized scoring, and whether its result would change a treatment decision today. Table 7 proposes a minimum dataset for an integrated precision immunopathology report, distinguishing items that can be reported in every case today from items recommended in selected settings or within clinical trials.

Table 6. Evidence-graded overview of candidate biomarkers and assays for an integrated precision immunopathology assessment of classic Hodgkin lymphoma.

Biomarker/Assay	Clinical Question	Level of Evidence	FFPE Feasibility/ Turnaround/ Standardized Scoring	Changes Treatment Decision Today?	Readiness Tier	Ref.
Morphology + standard IHC panel (CD30, CD15, PAX5, CD20, CD79a, OCT2, BOB.1, MUM1)	Diagnosis; subtyping	Guideline-endorsed (WHO-HAEM5, ICC)	Yes/1–3 days/ standardized	Yes (diagnosis)	Routine	[7,9,10]
EBER in situ hybridization	Diagnosis; EBV status	Guideline-endorsed (diagnostic); prognostic value inconsistent	Yes/1–2 days/ standardized	No (as prognostic marker)	Routine	[9,43,44]
Clinical scores (early-stage risk factors, IPS, A-HIPI)	Frontline risk stratification	Guideline-endorsed (risk factors, IPS); externally validated (A-HIPI)	Not tissue-based/immediate	Yes (treatment intensity)	Routine	[6,11–13]
Interim PET (Deauville score)	Response adaptation	Prospective, trial-embedded; guideline-endorsed	Imaging/during therapy/standardized	Yes	Routine	[15,16]
Baseline MTV	Frontline risk stratification	Retrospective analyses of prospective trials	Imaging/immediate/ partially standardized (segmentation methods vary)	No	Clinically validated, non-routine	[14]
Serum/plasma TARC (CCL17)	Early response; monitoring	Prospective cohorts; trial-embedded correlative analyses (SWOG S0816, HD0607)	Blood/hours/ commercial assays; no harmonized cut-off	No	Clinically validated, non-routine	[100–103]
ctDNA (genotyping, molecular tumor burden, MRD)	Baseline risk; early response; MRD; genomic subtype	Retrospective and prospective cohorts; trial-embedded (GHSG trials; S1826, abstract)	Plasma/ 1–3 weeks/not standardized	No (outside trials)	Clinically validated, non-routine/ investigational	[82,85–89]
PD-L1 IHC on HRS cells	Predicting benefit from PD-1 blockade	Retrospective, trial-correlative (CheckMate 205)	Yes/1–2 days/ no validated scoring system or cut-off in cHL	No	Investigational	[18,49]
9p24.1 FISH	Prognosis; predicting benefit from PD-1 blockade	Retrospective and trial-correlative	Yes/3–7 days/ research scoring criteria; no cut-off	No	Investigational	[18,49]
β2M/MHC class I and MHC class II IHC	Prognosis (chemotherapy); predicting benefit from PD-1 blockade (MHC-II)	Retrospective and trial-correlative	Yes/1–2 days/scoring not standardized	No	Investigational	[20,49,50]

Table 6. *Cont.*

Biomarker/Assay	Clinical Question	Level of Evidence	FFPE Feasibility/ Turnaround/ Standardized Scoring	Changes Treatment Decision Today?	Readiness Tier	Ref.
Macrophage markers (CD68/CD163); Treg:cytotoxic ratio	Prognosis	Retrospective (one trial-embedded study, E2496); inconsistent thresholds	Yes/1–2 days/ not standardized	No	Investigational	[48,51–54,57]
Multiplex and spatial immunoprofiling (mIF, cyclic IF, IMC, DSP, spatial transcriptomics)	Prognosis; resistance mechanisms; candidate predictors	Discovery; retrospective validation (e.g., RHL4S)	Partly (FFPE)/weeks/ platform-specific, not standardized	No	Investigational	[1,2,24–29]
Single-cell and peripheral immune profiling	Mechanisms of response/resistance to PD-1 blockade	Discovery	Fresh tissue or blood/weeks/ not standardized	No	Investigational	[30,31,66,68]
Digital image analysis/AI	Standardized quantification; prognosis	Discovery; retrospective, one or two centers, without external validation	Yes (WSI)/variable/not standardized; no approved cHL tool	No	Investigational	[39,78,79]

Readiness tiers: routine, established in routine practice; clinically validated, non-routine, supported by trial-embedded or independently validated data but not required for treatment decisions; investigational, research use only. Turnaround times are indicative. Abbreviations: A-HIPI, Advanced-Stage Hodgkin Lymphoma International Prognostic Index; DSP, digital spatial profiling; IMC, imaging mass cytometry; IPS, International Prognostic Score; MRD, minimal residual disease; MTV, metabolic tumor volume.

Table 7. Proposed minimum dataset for an integrated precision immunopathology report in classic Hodgkin lymphoma.

Report Section	Items	When/Readiness
A. Core diagnostic data	Specimen type and adequacy; histological subtype (WHO-HAEM5/ICC); HRS-cell immunophenotype (CD30, CD15, PAX5, CD20, CD79a, OCT2/BOB.1, MUM1, CD45); EBER status; exclusion of mimics; identification of FFPE block(s) suitable for further testing	Every case; routine
B. Clinical and imaging context	Stage; early-stage risk factors or IPS/A-HIPI; baseline PET-CT (MTV where available); interim PET result when available	Every case; routine (integrated from clinical record)
C. Extended tissue biomarkers	PD-L1 on HRS cells (IHC) and 9p24.1 status (FISH); β2M/MHC class I and MHC class II expression on HRS cells; macrophage and T-cell composition. Each reported with assay, antibody clone, and scoring method, and with an explicit statement that the result is not required for treatment selection	Selected cases or clinical trials; investigational
D. Plasma biomarkers	ctDNA (assay; baseline level; genomic subtype; on-treatment molecular response; MRD); serum TARC/CCL17	Clinical trials or prospective studies; clinically validated, non-routine
E. Spatial and computational data	Spatial neighborhood metrics, spatial scores, AI-derived quantification—reported separately and labeled as research results	Research only
F. Integrated interpretation	Synthesis of sections A–D, each item labeled by level of evidence; banking of tissue and plasma at diagnosis, given the move of PD-1 blockade to first-line therapy	Every case (sections A–B); expanded as evidence accrues

Abbreviations as in Table 6. Section C–E items should not be used to withhold approved therapies.

Such a workflow remains largely aspirational in routine diagnostic laboratories today, constrained by cost, turnaround time, the absence of harmonized analytical standards across spatial and computational platforms, and the need for prospective clinical validation before any single biomarker combination can be considered standard of care. Nonetheless, the trajectory of the field, and the broadly concordant findings emerging from complementary and independently developed technologies, make this integration a realistic goal, provided that the practical barriers discussed in Section 9 are addressed.

A further, practical consideration is where in the diagnostic pathway each layer should be deployed. Morphology and the standard immunohistochemical panel are appropriately

universal, applied to every new diagnosis. Extended immune, spatial, and molecular profiling, by contrast, is more realistically deployed selectively—within clinical trials designed specifically to validate candidate biomarkers, at relapse, or in diagnostically challenging cases—until evidence, cost, and turnaround time become compatible with universal application. Because PD-1 blockade has moved into first-line therapy, however, the diagnostic biopsy has become the key time-point for any biomarker intended to predict benefit from checkpoint blockade, so that the argument for reserving extended profiling for relapse no longer fully applies. At a minimum, adequate tissue (and, where possible, plasma) should be banked at diagnosis and the core dataset in Table 7 reported, so that extended assays can be performed later or within trials. Framed this way, precision immunopathology is not a wholesale replacement of conventional practice but a tiered extension of it, in which the depth of biological characterization is matched to the clinical question actually being asked.

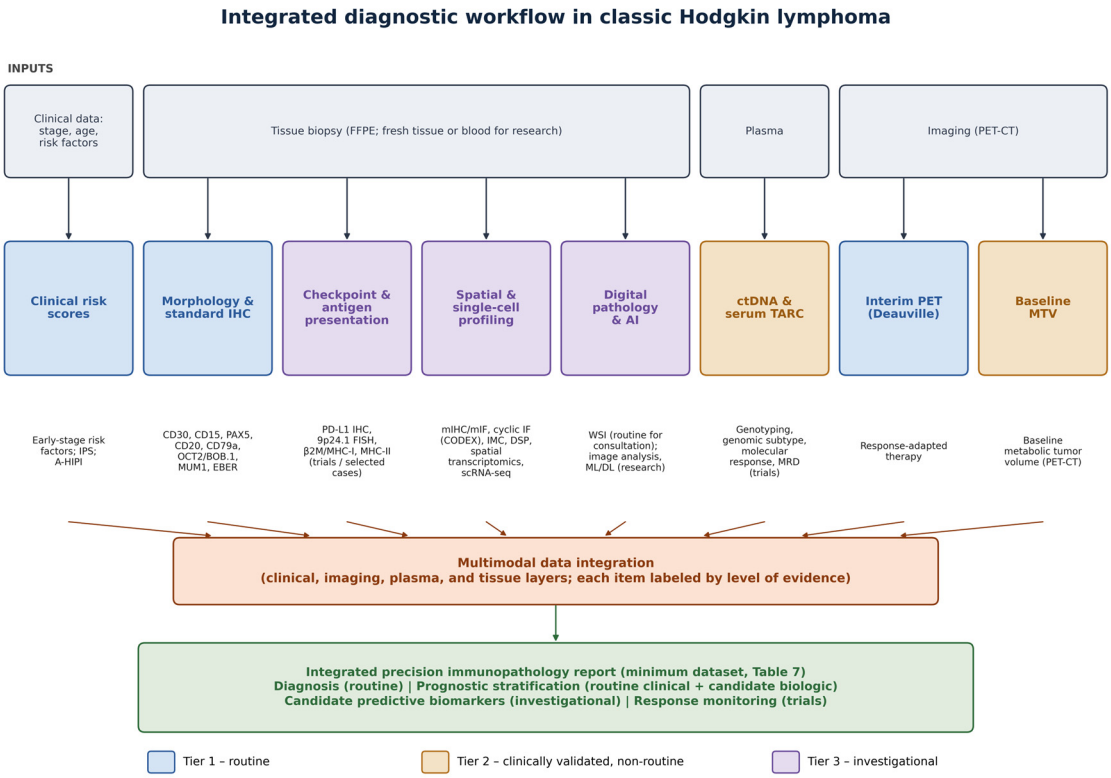


Figure 4. Proposed integrated diagnostic workflow for classic Hodgkin lymphoma. Clinical, tissue, plasma, and imaging inputs feed eight modules, color-coded by clinical readiness: tier 1, routine (clinical risk scores [6,11–13]; morphology and standard immunohistochemistry [7,9,10]; interim PET [15,16]); tier 2, clinically validated but non-routine (ctDNA and serum TARC [82,85–89,100–103]; baseline metabolic tumor volume [14]); tier 3, investigational (checkpoint and antigen-presentation assessment [18,49]; spatial and single-cell profiling [1,2,24–31,68]; digital pathology and AI [39,78,79]). Integration of these layers into a single report (minimum dataset in Table 7) is a proposed framework; except for tier 1 components, its elements are not currently required for treatment decisions.

9. Practical Barriers to Implementation

Translating the proposed framework into routine practice faces several concrete barriers. (i) Tissue requirements: HRS cells are rare, core-needle biopsies are increasingly used instead of excisional biopsies, and each additional assay consumes FFPE material that may be needed for diagnosis; multiplexed assays on a single section and ctDNA-based profiling partly mitigate this limitation. (ii) Assay reproducibility and inter-platform variability: PD-L1 and MHC immunohistochemistry lack cHL-specific validated clones, scoring algorithms

(HRS cells versus microenvironment), and cut-offs, while spatial and ctDNA platforms use different panels, chemistries, and analytical pipelines, so that results are not directly comparable across laboratories. (iii) Computational infrastructure: whole-slide imaging, multiplexed imaging, and sequencing generate large data volumes that require dedicated storage, image-management systems, bioinformatic expertise, and data-protection frameworks. (iv) Cost and cost-effectiveness: no formal health-economic evaluation of extended profiling in cHL is available, and in a highly curable disease the incremental value of any biomarker must be weighed against its cost. (v) Turnaround time: while standard immunohistochemistry is available within days, FISH, NGS, ctDNA, and spatial assays require one to several weeks, which is difficult to reconcile with the need to start treatment promptly. (vi) Regulatory validation: most extended assays are laboratory-developed tests that would require analytical and clinical validation under current regulatory frameworks (e.g., the European In Vitro Diagnostic Regulation) before clinical use, and computational tools face additional requirements as medical-device software. (vii) Availability and equity: spatial, single-cell, and AI platforms are currently confined to specialized academic centers, creating a risk of inequitable access unless centralized testing, external quality assessment programs, and training initiatives are developed.

Against this background, the components of the framework can be grouped by realistic time horizon (Table 6). Implementable today are morphology and the standard immunohistochemical panel, EBER in situ hybridization, clinical risk scores, interim PET-based response assessment, and whole-slide imaging for consultation and quality assurance. Clinically validated but not yet routine—and therefore suited to prospective trials and selected centers—are ctDNA-based response assessment, baseline metabolic tumor volume, and serum TARC. Investigational, and therefore confined to clinical trials and correlative studies, are PD-L1, 9p24.1, and MHC class I/II assessment as candidate predictors of benefit from PD-1 blockade, macrophage and T-cell composition, spatial immunoprofiling, single-cell technologies, and AI-based biomarkers; spatial, single-cell, and AI-based tools in particular are likely to remain research tools for the foreseeable future, until standardized, externally validated, and cost-effective versions become available.

To make the framework usable in routine practice, Table 8 translates it into a scenario-based testing algorithm. A core panel—morphology, the standard immunohistochemical panel (CD30, CD15, PAX5, CD20, CD79a, CD45, and MUM1, with OCT2/BOB.1 when needed), and EBER in situ hybridization—should be applied to every new diagnosis; together with stage, clinical risk scores, and PET, it is currently the only component whose results change clinical management. Additional analyses are warranted in defined scenarios: diagnostically challenging cases, in which extended immunohistochemistry and clonality or other molecular studies are chosen according to the differential diagnosis; limited samples, such as core-needle or pediatric biopsies, in which the core panel should be prioritized and residual material banked; relapsed or refractory disease, in which re-biopsy is needed to confirm relapse and exclude a different lymphoma; and clinical trials, in which extended tissue, plasma, spatial, and computational biomarkers should be collected prospectively. As regards resources, each immunohistochemical or FISH assay requires one 3–4 μm section; standard immunohistochemistry is available within one to three days and FISH within about one week, whereas NGS, ctDNA, and spatial assays require one to several weeks and entail considerably higher costs. Moreover, because HRS cells account for only about 1–5% of the cellularity, bulk tissue sequencing has limited sensitivity, and HRS-cell enrichment or ctDNA is generally required for genotyping [1,2,22,82].

Before any extended biomarker is recommended for routine adoption, three levels of evidence should be met. First, analytical validity: a locked assay with a defined antibody clone or probe, scoring method (HRS cells versus microenvironment), and cut-

off, with demonstrated intra- and inter-laboratory reproducibility, participation in external quality assessment, and compliance with accreditation and regulatory requirements. Second, clinical validity: independent validation of the prespecified cut-off in trial-based cohorts treated with contemporary regimens. Third, clinical utility: evidence that using the result changes management and improves outcome or reduces toxicity—for a predictive biomarker, a significant treatment-by-biomarker interaction in a randomized trial, established prospectively or through a prospective–retrospective analysis of archived trial specimens [70,71]—together with acceptable turnaround time, tissue consumption, and cost-effectiveness. None of the extended tissue biomarkers discussed in this review currently meets all three criteria.

Table 8. Proposed scenario-based testing algorithm for classic Hodgkin lymphoma: core panel, clinical scenarios warranting additional analyses, and results expected to change management.

Clinical Scenario	Recommended Testing	Results that May Change Management Today	Readiness	Ref.
Every new diagnosis (core panel)	Morphology; IHC for CD30, CD15, PAX5, CD20, CD79a, CD45, MUM1 (OCT2/BOB.1 as needed); EBER ISH; stage, clinical risk scores (early-stage risk factors, IPS/A-HIPI), baseline and interim PET	Yes: diagnosis and histological subtype; exclusion of mimics (e.g., NLPBCL); stage-, risk-, and PET-adapted therapy	Routine; required	[7,9–13,15,16]
Diagnostically challenging cases (e.g., differential diagnosis with large B-cell lymphomas, mediastinal gray-zone lymphoma, anaplastic large-cell lymphoma, or T-cell lymphomas with HRS-like cells)	Extended IHC, B- and T-cell clonality, and other molecular studies selected according to the differential diagnosis; expert hematopathology review	Yes: diagnosis (and therefore therapy)	Routine in selected cases	[9,10,41]
Limited tissue (core-needle biopsy; pediatric patients)	Prioritize the core panel; avoid consuming the block with non-essential assays; bank residual FFPE tissue and, where possible, plasma; ctDNA only within studies	Yes: diagnosis only	Routine (core panel); banking recommended	[87,88]
Advanced-stage disease: frontline choice between N-AVD, BV-AVD, and BrECADD (according to regional approval and availability)	No tissue biomarker required; PD-L1, 9p24.1, MHC class II, and ctDNA only within clinical trials; bank tissue and plasma at diagnosis	No (beyond core panel, clinical risk, and PET data)	Extended biomarkers investigational	[49,75,93–98]
Relapsed or refractory disease	Re-biopsy with core panel to confirm cHL and exclude another lymphoma; PD-L1, 9p24.1, MHC class II, and spatial scores (e.g., RHL4S) only within trials	Yes: confirmation of relapse; extended biomarkers: no	Core: routine; extended: investigational	[25,49]
Immunodeficiency-associated cHL (e.g., HIV-associated)	Core panel including EBER ISH; exclusion of other EBV-driven lymphoproliferations	Yes: diagnosis	Routine	[9,42]
Clinical trials and translational studies	Minimum dataset sections C–E (Table 7): PD-L1, 9p24.1 FISH, MHC class I/II, microenvironment composition; serial ctDNA and TARC; spatial and AI-based analyses	No (outside trials); aim is prospective validation	Clinically validated, non-routine/ investigational	[49,82,85–89,100–103]

Turnaround times, tissue requirements, and readiness tiers of individual assays are given in Table 6, and the corresponding report content in Table 7. Extended biomarkers should not delay treatment or be used to withhold approved therapies. Abbreviations: BV, brentuximab vedotin; FFPE, formalin-fixed, paraffin-embedded; IHC, immunohistochemistry; ISH, in situ hybridization; NLPBCL, nodular lymphocyte-predominant B-cell lymphoma; RHL4S, four-parameter spatial score (see Section 4); other abbreviations as in Table 6. Regulatory approval, labeled indications, and availability of N-AVD, BV-AVD, and BrECADD differ between regions (Section 7); the algorithm should be applied according to local approvals and guidelines.

10. Specific Clinical Populations

The framework may need adaptation in specific patient populations whose tumor biology and clinical context differ. In children, adolescents, and young adults, nodular sclerosis predominates, EBV positivity varies widely with geography and socioeconomic setting, diagnostic tissue is often limited, and late toxicity is a paramount concern; non-invasive ctDNA-based genotyping is particularly attractive in this setting [87,88], and adolescents enrolled in S1826 derived a sustained progression-free survival benefit from N-AVD [93]. In older patients, cHL is more frequently EBV-positive and of mixed cellularity subtype, the microenvironment and the prognostic weight of EBV status differ from those in younger adults [44], comorbidities limit treatment intensity, and N-AVD has shown particular benefit and better tolerability compared with brentuximab vedotin-AVD [94]; biomarkers that identify patients who can be cured with less toxic regimens are especially needed. Finally, immunodeficiency-associated cHL, most notably in people living with HIV, is almost invariably EBV-positive, is enriched for mixed cellularity and lymphocyte-depleted subtypes, and displays a distinct microenvironment shaped by systemic immune dysfunction [42]; the fifth edition of the WHO classification groups lymphoid proliferations and lymphomas arising in the setting of immune deficiency/dysregulation within a dedicated framework [9]. In these patients, checkpoint expression, antigen presentation, and T-cell composition may have a different meaning, and data on biomarker-guided immunotherapy remain very limited.

11. Conclusions and Future Perspectives

cHL has evolved, within little more than a decade and a half, from a disease diagnosed almost exclusively by morphology and a narrow immunohistochemical panel into a paradigm for immune-microenvironment-driven oncology. Discovery of near-universal 9p24.1 copy-number alterations, CIITA fusions, B2M mutations, and constitutive NF-κB/JAK-STAT activation gave a molecular explanation for the immune evasion long inferred from morphology alone, while multiplex immunohistochemistry, imaging mass cytometry, digital spatial profiling, spatial transcriptomics, and single-cell sequencing have provided the tools to visualize that evasion directly within intact tissue architecture. Digital pathology and artificial intelligence may offer a path to reproducible, scalable quantification of these multidimensional data, and ctDNA genotyping extends molecular characterization beyond the confines of tissue biopsy into non-invasive, longitudinal disease monitoring. Together, these advances define precision immunopathology: an ecosystem-centered diagnostic model that complements, rather than replaces, conventional pathology. Apart from the conventional diagnostic panel, however, none of the biomarkers discussed here is currently required to select patients for checkpoint blockade or CD30-directed therapy, and most remain prognostic associations or investigational tools; their future value will lie in refining risk stratification and, once prospectively validated, in guiding treatment de-escalation, escalation, or alternative strategies, now that PD-1 blockade has entered first-line therapy.

Realizing the full potential of this framework will require prospective, multicenter validation of candidate spatial, molecular, and plasma biomarkers—ideally embedded in frontline trials of regimens such as N-AVD and BrECADD—harmonization of pre-analytical and computational standards across platforms, and close collaboration between hematopathologists, molecular biologists, and computational scientists. If successful, such an effort promises to make cHL one of the first lymphoid malignancies in which routine diagnostic pathology is fully integrated with the biology of the tumor-immune ecosystem that it has, in practice, always been describing.

Author Contributions: A.C. Designed the work and supervised the paper; C.C.V. Wrote the paper and prepared Figures 2 and 3; D.V.T. Reviewed the manuscript and contributed to the editing and accuracy of the English; A.G. wrote the paper and designed the figures. All authors have read and agreed to the published version of the manuscript.

Funding: This research received no external funding.

Data Availability Statement: The raw data supporting the conclusions of this article will be made available by the authors on request.

Acknowledgments: The authors used Claude (Anthropic, San Francisco, CA, USA; Opus 5.5) for English-language editing, for generating the graphical layout of Figures 1 and 4 (original and revised versions), and for redrawing the revised Figures 2 and 3 from the original author-drawn figures. For all figures, the scientific content—cell populations, molecular alterations, relationships depicted, and text labels—was specified by the authors, and every element was checked by the authors against the cited sources. The authors have reviewed and edited all output and take full responsibility for the content of this publication.

Conflicts of Interest: The authors declare no conflicts of interest.

Abbreviations

The following abbreviations are used in this manuscript:

A-HIPI	Advanced-Stage Hodgkin Lymphoma International Prognostic Index
ADC	Antibody-drug conjugate
AI	Artificial intelligence
ASCT	Autologous stem-cell transplantation
AVD	Doxorubicin, vinblastine, dacarbazine
B2M	Beta-2-microglobulin
BV	Brentuximab vedotin
cHL	Classic Hodgkin lymphoma
CNN	Convolutional neural network
CODEX	Co-detection by indexing
ctDNA	Circulating tumor DNA
CyTOF	Cytometry by time of flight (mass cytometry)
DSP	Digital spatial profiling
EBER	Epstein–Barr virus-encoded small RNA
EBV	Epstein–Barr virus
FDA	Food and Drug Administration
FFPE	Formalin-fixed, paraffin-embedded
FISH	Fluorescence in situ hybridization
HRS	Hodgkin and Reed–Sternberg
ICC	International Consensus Classification
IHC	Immunohistochemistry
IMC	Imaging mass cytometry
IPS	International Prognostic Score
LMP1	Latent membrane protein 1
MHC	Major histocompatibility complex
mIHC/mIF	Multiplex immunohistochemistry/immunofluorescence
ML/DL	Machine learning/deep learning
MMAE	Monomethyl auristatin E
MRD	Minimal residual disease
MTV	Metabolic tumor volume
N-AVD	Nivolumab plus doxorubicin, vinblastine, dacarbazine
NF-κB	Nuclear factor kappa-light-chain-enhancer of activated B cells
NGS	Next-generation sequencing

NK	Natural killer
NLPBCL	Nodular lymphocyte-predominant B-cell lymphoma
PD-1	Programmed cell death protein 1
PD-L1	Programmed death-ligand 1
PD-L2	Programmed death-ligand 2
PET-CT	Positron emission tomography–computed tomography
PFS	Progression-free survival
R/R	Relapsed/refractory
scRNA-seq	Single-cell RNA sequencing
TAMs	Tumor-associated macrophages
TARC	Thymus and activation-regulated chemokine (CCL17)
TME	Tumor microenvironment
Tregs	Regulatory T cells
WHO	World Health Organization
WSI	Whole-slide imaging

References

1. Pourmaleki, M.; Jones, C.J.; Mellinghoff, S.D.; Greenstein, B.D.; Kumar, P.; Foronda, M.; Navarrete, D.A.; Campos, C.; Roshal, M.; Schultz, N.; et al. Multiplexed Spatial Profiling of Hodgkin Reed-Sternberg Cell Neighborhoods in Classic Hodgkin Lymphoma. *Clin. Cancer Res.* **2024**, *30*, 3881–3893. [CrossRef] [PubMed]
2. Shanmugam, V.; Tokcan, N.; Chafamo, D.; Sullivan, S.; Borji, M.; Martin, H.; Newton, G.; Nadaf, N.; Hanbury, S.; Barrera, I.; et al. Genome-scale spatial mapping of the Hodgkin lymphoma microenvironment identifies tumor cell survival factors. *Nat. Commun.* **2026**, *17*, 838. Correction in *Nat. Commun.* **2026**, *17*, 4813. https://doi.org/10.1038/s41467-026-73753-2. [CrossRef] [PubMed]
3. Küppers, R. The biology of Hodgkin's lymphoma. *Nat. Rev. Cancer* **2009**, *9*, 15–27. [CrossRef] [PubMed]
4. Weniger, M.A.; Küppers, R. Molecular biology of Hodgkin lymphoma. *Leukemia* **2021**, *35*, 968–981. [CrossRef] [PubMed]
5. Shanbhag, S.; Ambinder, R.F. Hodgkin lymphoma: A review and update on recent progress. *CA Cancer J. Clin.* **2018**, *68*, 116–132. [CrossRef] [PubMed]
6. Ansell, S.M. Hodgkin lymphoma: 2023 update on diagnosis, risk-stratification, and management. *Am. J. Hematol.* **2022**, *97*, 1478–1488. [CrossRef] [PubMed]
7. Satou, A.; Takahara, T.; Nakamura, S. An Update on the Pathology and Molecular Features of Hodgkin Lymphoma. *Cancers* **2022**, *14*, 2647. [CrossRef] [PubMed]
8. Swerdlow, S.H.; Campo, E.; Pileri, S.A.; Harris, N.L.; Stein, H.; Siebert, R.; Advani, R.; Ghielmini, M.; Salles, G.A.; Zelenetz, A.D.; et al. The 2016 revision of the World Health Organization classification of lymphoid neoplasms. *Blood* **2016**, *127*, 2375–2390. [CrossRef] [PubMed]
9. Alaggio, R.; Amador, C.; Anagnostopoulos, I.; Attygalle, A.D.; Araujo, I.B.O.; Berti, E.; Bhagat, G.; Borges, A.M.; Boyer, D.; Calaminici, M.; et al. The 5th edition of the World Health Organization Classification of Haematolymphoid Tumours: Lymphoid Neoplasms. *Leukemia* **2022**, *36*, 1720–1748. [CrossRef] [PubMed]
10. Campo, E.; Jaffe, E.S.; Cook, J.R.; Quintanilla-Martinez, L.; Swerdlow, S.H.; Anderson, K.C.; Brousset, P.; Cerroni, L.; de Leval, L.; Dirnhofer, S.; et al. The International Consensus Classification of Mature Lymphoid Neoplasms: A report from the Clinical Advisory Committee. *Blood* **2022**, *140*, 1229–1253. [CrossRef] [PubMed]
11. Hasenclever, D.; Diehl, V. A prognostic score for advanced Hodgkin's disease. International Prognostic Factors Project on Advanced Hodgkin's Disease. *N. Engl. J. Med.* **1998**, *339*, 1506–1514. [CrossRef] [PubMed]
12. Rodday, A.M.; Parsons, S.K.; Upshaw, J.N.; Friedberg, J.W.; Gallamini, A.; Hawkes, E.; Hodgson, D.; Johnson, P.; Link, B.K.; Mou, E.; et al. The Advanced-Stage Hodgkin Lymphoma International Prognostic Index: Development and Validation of a Clinical Prediction Model From the HoLISTIC Consortium. *J. Clin. Oncol.* **2023**, *41*, 2076–2086. [CrossRef] [PubMed]
13. Tharmaseelan, H.; Jablonski, J.; Parsons, S.K.; Rodday, A.M.; Evens, A.M.; Zijlstra, J.M.; Fosså, A.; Molin, D.; Hertzberg, M.; Hitz, F.; et al. Validation of the advanced-stage Hodgkin lymphoma international prognostic index (A-HIPI) in the GHSG HD21 trial. *Hemasphere* **2026**, *10*, e70471. [CrossRef] [PubMed]
14. Cottereau, A.S.; Versari, A.; Loft, A.; Casasnovas, O.; Bellei, M.; Ricci, R.; Bardet, S.; Castagnoli, A.; Brice, P.; Raemaekers, J.; et al. Prognostic value of baseline metabolic tumor volume in early-stage Hodgkin lymphoma in the standard arm of the H10 trial. *Blood* **2018**, *131*, 1456–1463. [CrossRef] [PubMed]

15. Johnson, P.; Federico, M.; Kirkwood, A.; Fosså, A.; Berkahn, L.; Carella, A.; d'Amore, F.; Enblad, G.; Franceschetto, A.; Fulham, M.; et al. Adapted Treatment Guided by Interim PET-CT Scan in Advanced Hodgkin's Lymphoma. *N. Engl. J. Med.* **2016**, *374*, 2419–2429. [CrossRef] [PubMed]
16. Press, O.W.; Li, H.; Schöder, H.; Straus, D.J.; Moskowitz, C.H.; LeBlanc, M.; Rimsza, L.M.; Bartlett, N.L.; Evens, A.M.; Mittra, E.S.; et al. US Intergroup Trial of Response-Adapted Therapy for Stage III to IV Hodgkin Lymphoma Using Early Interim Fluorodeoxyglucose-Positron Emission Tomography Imaging: Southwest Oncology Group S0816. *J. Clin. Oncol.* **2016**, *34*, 2020–2027. [CrossRef] [PubMed]
17. Green, M.R.; Monti, S.; Rodig, S.J.; Juszczynski, P.; Currie, T.; O'Donnell, E.; Chapuy, B.; Takeyama, K.; Neuberg, D.; Golub, T.R.; et al. Integrative analysis reveals selective 9p24.1 amplification, increased PD-1 ligand expression, and further induction via JAK2 in nodular sclerosing Hodgkin lymphoma and primary mediastinal large B-cell lymphoma. *Blood* **2010**, *116*, 3268–3277. [CrossRef] [PubMed]
18. Roemer, M.G.; Advani, R.H.; Ligon, A.H.; Natkunam, Y.; Redd, R.A.; Homer, H.; Connelly, C.F.; Sun, H.H.; Daadi, S.E.; Freeman, G.J.; et al. PD-L1 and PD-L2 Genetic Alterations Define Classical Hodgkin Lymphoma and Predict Outcome. *J. Clin. Oncol.* **2016**, *34*, 2690–2697. [CrossRef] [PubMed]
19. Steidl, C.; Shah, S.P.; Woolcock, B.W.; Rui, L.; Kawahara, M.; Farinha, P.; Johnson, N.A.; Zhao, Y.; Telenius, A.; Neriah, S.B.; et al. MHC class II transactivator CIITA is a recurrent gene fusion partner in lymphoid cancers. *Nature* **2011**, *471*, 377–381. [CrossRef] [PubMed]
20. Roemer, M.G.; Advani, R.H.; Redd, R.A.; Pinkus, G.S.; Natkunam, Y.; Ligon, A.H.; Connelly, C.F.; Pak, C.J.; Carey, C.D.; Daadi, S.E.; et al. Classical Hodgkin Lymphoma with Reduced β2M/MHC Class I Expression Is Associated with Inferior Outcome Independent of 9p24.1 Status. *Cancer Immunol. Res.* **2016**, *4*, 910–916. [CrossRef] [PubMed]
21. Jardin, F. NFkB Pathway and Hodgkin Lymphoma. *Biomedicines* **2022**, *10*, 2153. [CrossRef] [PubMed]
22. Wienand, K.; Chapuy, B.; Stewart, C.; Dunford, A.J.; Wu, D.; Kim, J.; Kamburov, A.; Wood, T.R.; Cader, F.Z.; Ducar, M.D.; et al. Genomic analyses of flow-sorted Hodgkin Reed-Sternberg cells reveal complementary mechanisms of immune evasion. *Blood Adv.* **2019**, *3*, 4065–4080. [CrossRef] [PubMed]
23. Reichel, J.; Chadburn, A.; Rubinstein, P.G.; Giulino-Roth, L.; Tam, W.; Liu, Y.; Gaiolla, R.; Eng, K.; Brody, J.; Inghirami, G.; et al. Flow sorting and exome sequencing reveal the oncogenome of primary Hodgkin and Reed-Sternberg cells. *Blood* **2015**, *125*, 1061–1072. [CrossRef] [PubMed]
24. Carbone, A.; Gloghini, A.; Pruneri, G.; Dolcetti, R. Optimizing checkpoint inhibitors therapy for relapsed or progressive classic Hodgkin lymphoma by multiplex immunohistochemistry of the tumor microenvironment. *Cancer Med.* **2019**, *8*, 3012–3016. [CrossRef] [PubMed]
25. Aoki, T.; Jiang, A.; Xu, A.; Yin, Y.; Gamboa, A.; Milne, K.; Takata, K.; Miyata-Takata, T.; Chung, S.; Rai, S.; et al. Spatially Resolved Tumor Microenvironment Predicts Treatment Outcomes in Relapsed/Refractory Hodgkin Lymphoma. *J. Clin. Oncol.* **2024**, *42*, 1077–1087. [CrossRef] [PubMed]
26. Merritt, C.R.; Ong, G.T.; Church, S.E.; Barker, K.; Danaher, P.; Geiss, G.; Hoang, M.; Jung, J.; Liang, Y.; McKay-Fleisch, J.; et al. Multiplex digital spatial profiling of proteins and RNA in fixed tissue. *Nat. Biotechnol.* **2020**, *38*, 586–599. [CrossRef] [PubMed]
27. Takeuchi, M.; Miyoshi, H.; Semba, Y.; Yamada, K.; Nakashima, K.; Sato, K.; Furuta, T.; Moritsubo, M.; Ogura, Y.; Tanaka, K.; et al. Digital spatial profiling of $CD4^+$ T cells in classic Hodgkin lymphoma. *Virchows Arch.* **2023**, *483*, 255–260. [CrossRef] [PubMed]
28. Pickard, K.; Stephenson, E.; Mitchell, A.; Jardine, L.; Bacon, C.M. Location, location, location: Mapping the lymphoma tumor microenvironment using spatial transcriptomics. *Front. Oncol.* **2023**, *13*, 1258245. [CrossRef] [PubMed]
29. Alonso-Alonso, R.; Menendez, V.; Vázquez, E.M.; Solórzano, J.L.; García, J.F. The Hodgkin Lymphoma Microenvironment: Insights from Spatial Transcriptomics. *Int. J. Mol. Sci.* **2026**, *27*, 3689. [CrossRef] [PubMed]
30. Cader, F.Z.; Schackmann, R.C.J.; Hu, X.; Wienand, K.; Redd, R.; Chapuy, B.; Ouyang, J.; Paul, N.; Gjini, E.; Lipschitz, M.; et al. Mass cytometry of Hodgkin lymphoma reveals a $CD4^+$ regulatory T-cell-rich and exhausted T-effector microenvironment. *Blood* **2018**, *132*, 825–836. [CrossRef] [PubMed]
31. Aoki, T.; Chong, L.C.; Takata, K.; Milne, K.; Hav, M.; Colombo, A.; Chavez, E.A.; Nissen, M.; Wang, X.; Miyata-Takata, T.; et al. Single-Cell Transcriptome Analysis Reveals Disease-Defining T-cell Subsets in the Tumor Microenvironment of Classic Hodgkin Lymphoma. *Cancer Discov.* **2020**, *10*, 406–421. [CrossRef] [PubMed]
32. van den Brand, M.; Nooijen, P.; van der Laan, K.D.; de Bruin, P.C.; van Leeuwen, A.M.G.; Leeuwis, J.W.; Meijer, J.W.; Otte-Höller, I.; Hebeda, K.M. Discrepancies in digital hematopathology diagnoses for consultation and expert panel analysis. *Virchows Arch.* **2021**, *478*, 535–540. [CrossRef] [PubMed]
33. Syrykh, C.; Abreu, A.; Amara, N.; Siegfried, A.; Maisongrosse, V.; Frenois, F.X.; Martin, L.; Rossi, C.; Laurent, C.; Brousset, P. Accurate diagnosis of lymphoma on whole-slide histopathology images using deep learning. *npj Digit. Med.* **2020**, *3*, 63. [CrossRef] [PubMed]
34. Kang, M.; Yang, Z.; Yu, T.; Li, D.; Wang, Z.; Chen, L. Clinical applications of artificial intelligence in the histopathology of lymphoma: Diagnosis, treatment and prognosis. *Discov. Oncol.* **2025**, *16*, 2180. [CrossRef] [PubMed]

35. Bera, K.; Schalper, K.A.; Rimm, D.L.; Velcheti, V.; Madabhushi, A. Artificial intelligence in digital pathology—New tools for diagnosis and precision oncology. *Nat. Rev. Clin. Oncol.* **2019**, *16*, 703–715. [CrossRef] [PubMed]
36. Gloghini, A.; Carbone, A. Tumour Microenvironment Contribution to Checkpoint Inhibitor Therapy in Classic Hodgkin Lymphoma. *Hemato* **2024**, *5*, 199–207. [CrossRef]
37. Alibrahim, M.N.; Carbone, A.; Alsaleh, N.; Gloghini, A. Immune Checkpoint Molecules in Hodgkin Lymphoma and Other Hematological Malignancies. *Cancers* **2025**, *17*, 2292. [CrossRef] [PubMed]
38. Gloghini, A.; Lorenzini, D.; Volpi, C.C.; Trupia, D.V.; Pruneri, G. Hodgkin Reed-Sternberg Cells of Classic Hodgkin Lymphoma: Morphology, Phenotype, Genotype, and Cell of Origin. *Cancers* **2026**, *18*, 1446. [CrossRef] [PubMed]
39. Alibrahim, M.N.; Gloghini, A.; Carbone, A. How artificial intelligence may solve diagnostic and prognostic challenges in classic Hodgkin lymphoma. *Blood Rev.* **2026**, *77*, 101390. [CrossRef]
40. Alibrahim, M.N.; Carbone, A.; Gloghini, A. Predictors of sensitivity to immune therapies in classic Hodgkin lymphoma. *Blood Neoplasia* **2026**, *3*, 100207. [CrossRef] [PubMed]
41. Browne, P.; Petrosyan, K.; Hernandez, A.; Chan, J.A. The B-cell transcription factors BSAP, Oct-2, and BOB.1 and the pan-B-cell markers CD20, CD22, and CD79a are useful in the differential diagnosis of classic Hodgkin lymphoma. *Am. J. Clin. Pathol.* **2003**, *120*, 767–777. [CrossRef] [PubMed]
42. Carbone, A.; Vaccher, E.; Gloghini, A. Hematologic cancers in individuals infected by HIV. *Blood* **2022**, *139*, 995–1012. [CrossRef] [PubMed]
43. Santisteban-Espejo, A.; Perez-Requena, J.; Atienza-Cuevas, L.; Moran-Sanchez, J.; Fernandez-Valle, M.D.C.; Bernal-Florindo, I.; Romero-Garcia, R.; Garcia-Rojo, M. Prognostic Role of the Expression of Latent-Membrane Protein 1 of Epstein-Barr Virus in Classical Hodgkin Lymphoma. *Viruses* **2021**, *13*, 2523. [CrossRef] [PubMed]
44. Hu, J.; Zhang, X.; Tao, H.; Jia, Y. The prognostic value of Epstein-Barr virus infection in Hodgkin lymphoma: A systematic review and meta-analysis. *Front. Oncol.* **2022**, *12*, 1034398. [CrossRef] [PubMed]
45. van der Weyden, C.A.; Pileri, S.A.; Feldman, A.L.; Whisstock, J.; Prince, H.M. Understanding CD30 biology and therapeutic targeting: A historical perspective providing insight into future directions. *Blood Cancer J.* **2017**, *7*, e603. [CrossRef] [PubMed]
46. Li, Z.; Guo, W.; Bai, O. Mechanism of action and therapeutic targeting of CD30 molecule in lymphomas. *Front. Oncol.* **2023**, *13*, 1301437. [CrossRef] [PubMed]
47. Jacobsen, E.D.; Sharman, J.P.; Oki, Y.; Advani, R.H.; Winter, J.N.; Bello, C.M.; Spitzer, G.; Palanca-Wessels, M.C.; Kennedy, D.A.; Levine, P.; et al. Brentuximab vedotin demonstrates objective responses in a phase 2 study of relapsed/refractory DLBCL with variable CD30 expression. *Blood* **2015**, *125*, 1394–1402. [CrossRef] [PubMed]
48. Mavili, H.S.; Isisag, A.; Tan, A.; Miskioglu, M.; Baraz, L.S.; Nese, N. Relationship of Tumor-Associated Macrophage Population Detected by CD68 PG-M1, CD68 KP1, and CD163 with Latent EBV Infection and Prognosis in Classical Hodgkin Lymphoma. *Turk. Patoloji Derg.* **2021**, *37*, 130–138. [CrossRef] [PubMed]
49. Roemer, M.G.M.; Redd, R.A.; Cader, F.Z.; Pak, C.J.; Abdelrahman, S.; Ouyang, J.; Sasse, S.; Younes, A.; Fanale, M.; Santoro, A.; et al. Major Histocompatibility Complex Class II and Programmed Death Ligand 1 Expression Predict Outcome After Programmed Death 1 Blockade in Classic Hodgkin Lymphoma. *J. Clin. Oncol.* **2018**, *36*, 942–950. [CrossRef] [PubMed]
50. Diepstra, A.; van Imhoff, G.W.; Karim-Kos, H.E.; van den Berg, A.; te Meerman, G.J.; Niens, M.; Nolte, I.M.; Bastiaannet, E.; Schaapveld, M.; Vellenga, E.; et al. HLA class II expression by Hodgkin Reed-Sternberg cells is an independent prognostic factor in classical Hodgkin's lymphoma. *J. Clin. Oncol.* **2007**, *25*, 3101–3108. [CrossRef] [PubMed]
51. Steidl, C.; Lee, T.; Shah, S.P.; Farinha, P.; Han, G.; Nayar, T.; Delaney, A.; Jones, S.J.; Iqbal, J.; Weisenburger, D.D.; et al. Tumor-associated macrophages and survival in classic Hodgkin's lymphoma. *N. Engl. J. Med.* **2010**, *362*, 875–885. [CrossRef] [PubMed]
52. Tan, K.L.; Scott, D.W.; Hong, F.; Kahl, B.S.; Fisher, R.I.; Bartlett, N.L.; Advani, R.H.; Buckstein, R.; Rimsza, L.M.; Connors, J.M.; et al. Tumor-associated macrophages predict inferior outcomes in classic Hodgkin lymphoma: A correlative study from the E2496 Intergroup trial. *Blood* **2012**, *120*, 3280–3287. [CrossRef] [PubMed]
53. Harris, J.A.; Jain, S.; Ren, Q.; Zarineh, A.; Liu, C.; Ibrahim, S. *CD*163 versus CD68 in tumor associated macrophages of classical Hodgkin lymphoma. *Diagn. Pathol.* **2012**, *7*, 12. [CrossRef] [PubMed]
54. Karihtala, K.; Leivonen, S.K.; Brück, O.; Karjalainen-Lindsberg, M.L.; Mustjoki, S.; Pellinen, T.; Leppä, S. Prognostic Impact of Tumor-Associated Macrophages on Survival Is Checkpoint Dependent in Classical Hodgkin Lymphoma. *Cancers* **2020**, *12*, 877. [CrossRef] [PubMed]
55. Patel, S.S.; Weirather, J.L.; Lipschitz, M.; Lako, A.; Chen, P.H.; Griffin, G.K.; Armand, P.; Shipp, M.A.; Rodig, S.J. The microenvironmental niche in classic Hodgkin lymphoma is enriched for CTLA-4-positive T cells that are PD-1-negative. *Blood* **2019**, *134*, 2059–2069. [CrossRef] [PubMed]
56. Cellini, A.; Scarmozzino, F.; Angotzi, F.; Ruggeri, E.; Dei Tos, A.P.; Trentin, L.; Pizzi, M.; Visentin, A. Tackling the dysregulated immune-checkpoints in classical Hodgkin lymphoma: Bidirectional regulations between the microenvironment and Hodgkin/Reed-Sternberg cells. *Front. Oncol.* **2023**, *13*, 1203470. [CrossRef] [PubMed]

57. Kelley, T.W.; Pohlman, B.; Elson, P.; Hsi, E.D. The ratio of FOXP3+ regulatory T cells to granzyme B+ cytotoxic T/NK cells predicts prognosis in classical Hodgkin lymphoma and is independent of bcl-2 and MAL expression. *Am. J. Clin. Pathol.* **2007**, *128*, 958–965. [CrossRef] [PubMed]
58. Vardhana, S.; Younes, A. The immune microenvironment in Hodgkin lymphoma: T cells, B cells, and immune checkpoints. *Haematologica* **2016**, *101*, 794–802. [CrossRef] [PubMed]
59. Georgoulis, V.; Papoudou-Bai, A.; Makis, A.; Kanavaros, P.; Hatzimichael, E. Unraveling the Immune Microenvironment in Classic Hodgkin Lymphoma: Prognostic and Therapeutic Implications. *Biology* **2023**, *12*, 862. [CrossRef] [PubMed]
60. Veldman, J.; Visser, L.; Huberts-Kregel, M.; Muller, N.; Hepkema, B.; van den Berg, A.; Diepstra, A. Rosetting T cells in Hodgkin lymphoma are activated by immunological synapse components HLA class II and CD58. *Blood* **2020**, *136*, 2437–2441. [CrossRef] [PubMed]
61. van den Berg, A.; Visser, L.; Poppema, S. High expression of the CC chemokine TARC in Reed-Sternberg cells. A possible explanation for the characteristic T-cell infiltrate in Hodgkin's lymphoma. *Am. J. Pathol.* **1999**, *154*, 1685–1691. [CrossRef] [PubMed]
62. Juszczynski, P.; Ouyang, J.; Monti, S.; Rodig, S.J.; Takeyama, K.; Abramson, J.; Chen, W.; Kutok, J.L.; Rabinovich, G.A.; Shipp, M.A. The AP1-dependent secretion of galectin-1 by Reed Sternberg cells fosters immune privilege in classical Hodgkin lymphoma. *Proc. Natl. Acad. Sci. USA* **2007**, *104*, 13134–13139. [CrossRef] [PubMed]
63. Tamma, R.; Ingravallo, G.; Gaudio, F.; d'Amati, A.; Masciopinto, P.; Bellitti, E.; Lorusso, L.; Annese, T.; Benagiano, V.; Musto, P.; et al. The Tumor Microenvironment in Classic Hodgkin's Lymphoma in Responder and No-Responder Patients to First Line ABVD Therapy. *Cancers* **2023**, *15*, 2803. [CrossRef] [PubMed]
64. Gandhi, M.K.; Keane, C. CD4 T cells: The complicated key to unlocking the immune environment of classical Hodgkin lymphoma. *Haematologica* **2023**, *108*, 945–946. [CrossRef] [PubMed]
65. Karihtala, K.; Leivonen, S.K.; Karjalainen-Lindsberg, M.L.; Chan, F.C.; Steidl, C.; Pellinen, T.; Leppä, S. Checkpoint protein expression in the tumor microenvironment defines the outcome of classical Hodgkin lymphoma patients. *Blood Adv.* **2022**, *6*, 1919–1931. [CrossRef] [PubMed]
66. Cader, F.Z.; Hu, X.; Goh, W.L.; Wienand, K.; Ouyang, J.; Mandato, E.; Redd, R.; Lawton, L.N.; Chen, P.H.; Weirather, J.L.; et al. A peripheral immune signature of responsiveness to PD-1 blockade in patients with classical Hodgkin lymphoma. *Nat. Med.* **2020**, *26*, 1468–1479. [CrossRef] [PubMed]
67. Vari, F.; Arpon, D.; Keane, C.; Hertzberg, M.S.; Talaulikar, D.; Jain, S.; Cui, Q.; Han, E.; Tobin, J.; Bird, R.; et al. Immune evasion via PD-1/PD-L1 on NK cells and monocyte/macrophages is more prominent in Hodgkin lymphoma than DLBCL. *Blood* **2018**, *131*, 1809–1819. [CrossRef] [PubMed]
68. Paczkowska, J.; Tang, M.; Wright, K.T.; Song, L.; Luu, K.; Shanmugam, V.; Welsh, E.L.; Weirather, J.L.; Besson, N.; Olszewski, H.; et al. Cancer-specific innate and adaptive immune rewiring drives resistance to PD-1 blockade in classic Hodgkin lymphoma. *Nat. Commun.* **2024**, *15*, 10740. [CrossRef] [PubMed]
69. Jeong, A.R.; Ball, E.D.; Goodman, A.M. Predicting Responses to Checkpoint Inhibitors in Lymphoma: Are We Up to the Standards of Solid Tumors? *Clin. Med. Insights Oncol.* **2020**, *14*, 1179554920976366. [CrossRef] [PubMed]
70. Ballman, K.V. Biomarker: Predictive or Prognostic? *J. Clin. Oncol.* **2015**, *33*, 3968–3971. [CrossRef] [PubMed]
71. Simon, R.M.; Paik, S.; Hayes, D.F. Use of Archived Specimens in Evaluation of Prognostic and Predictive Biomarkers. *J. Natl. Cancer Inst.* **2009**, *101*, 1446–1452. [CrossRef] [PubMed]
72. Armand, P.; Engert, A.; Younes, A.; Fanale, M.; Santoro, A.; Zinzani, P.L.; Timmerman, J.M.; Collins, G.P.; Ramchandren, R.; Cohen, J.B.; et al. Nivolumab for Relapsed/Refractory Classic Hodgkin Lymphoma After Failure of Autologous Hematopoietic Cell Transplantation: Extended Follow-Up of the Multicohort Single-Arm Phase II CheckMate 205 Trial. *J. Clin. Oncol.* **2018**, *36*, 1428–1439. [CrossRef] [PubMed]
73. Chen, R.; Zinzani, P.L.; Fanale, M.A.; Armand, P.; Johnson, N.A.; Brice, P.; Radford, J.; Ribrag, V.; Molin, D.; Vassilakopoulos, T.P.; et al. Phase II Study of the Efficacy and Safety of Pembrolizumab for Relapsed/Refractory Classic Hodgkin Lymphoma. *J. Clin. Oncol.* **2017**, *35*, 2125–2132. [CrossRef] [PubMed]
74. Kuruvilla, J.; Ramchandren, R.; Santoro, A.; Paszkiewicz-Kozik, E.; Gasiorowski, R.; Johnson, N.A.; Fogliatto, L.M.; Goncalves, I.; de Oliveira, J.S.R.; Buccheri, V.; et al. Pembrolizumab versus brentuximab vedotin in relapsed or refractory classical Hodgkin lymphoma (KEYNOTE-204): An interim analysis of a multicentre, randomised, open-label, phase 3 study. *Lancet Oncol.* **2021**, *22*, 512–524. [CrossRef] [PubMed]
75. Herrera, A.F.; LeBlanc, M.; Castellino, S.M.; Li, H.; Rutherford, S.C.; Evens, A.M.; Davison, K.; Punnett, A.; Parsons, S.K.; Ahmed, S.; et al. Nivolumab+AVD in Advanced-Stage Classic Hodgkin's Lymphoma. *N. Engl. J. Med.* **2024**, *391*, 1379–1389. [CrossRef] [PubMed]
76. Ansell, S.M.; Lesokhin, A.M.; Borrello, I.; Halwani, A.; Scott, E.C.; Gutierrez, M.; Schuster, S.J.; Millenson, M.M.; Cattry, D.; Freeman, G.J.; et al. PD-1 blockade with nivolumab in relapsed or refractory Hodgkin's lymphoma. *N. Engl. J. Med.* **2015**, *372*, 311–319. [CrossRef] [PubMed]

77. Aoki, T.; Steidl, C. Novel insights into Hodgkin lymphoma biology by single-cell analysis. *Blood* **2023**, *141*, 1791–1801. [CrossRef] [PubMed]
78. Santisteban-Espejo, A.; Bernal-Florindo, I.; Perez-Requena, J.; Atienza-Cuevas, L.; Maira-Gonzalez, N.; Garcia-Rojo, M. Whole-slide image analysis identifies a high content of Hodgkin Reed-Sternberg cells and a low content of T lymphocytes in tumor microenvironment as predictors of adverse outcome in patients with classic Hodgkin lymphoma treated with ABVD. *Front. Oncol.* **2022**, *12*, 1000762. [CrossRef] [PubMed]
79. Motmaen, I.; Sereda, S.; Brobeil, A.; Shankar, A.; Braeuninger, A.; Hasenclever, D.; Gattenlöhner, S. Deep-learning based classification of a tumor marker for prognosis on Hodgkin's disease. *Eur. J. Haematol.* **2023**, *111*, 722–728. [CrossRef] [PubMed]
80. Uppal, A.; Kakkar, B.; Johri, P.; Kumar, Y.; Koul, A. Enhancing lymphoma cancer detection using deep transfer learning on histopathological images. *Sci. Rep.* **2025**, *15*, 38042. [CrossRef] [PubMed]
81. Mata, E.; Díaz-López, A.; Martín-Moreno, A.M.; Sánchez-Beato, M.; Varela, I.; Mestre, M.J.; Santonja, C.; Burgos, F.; Menárguez, J.; Estévez, M.; et al. Analysis of the mutational landscape of classic Hodgkin lymphoma identifies disease heterogeneity and potential therapeutic targets. *Oncotarget* **2017**, *8*, 111386–111395. [CrossRef] [PubMed]
82. Spina, V.; Bruscaggin, A.; Cuccaro, A.; Martini, M.; Di Trani, M.; Forestieri, G.; Manzoni, M.; Condoluci, A.; Arribas, A.; Terzi-Di-Bergamo, L.; et al. Circulating tumor DNA reveals genetics, clonal evolution, and residual disease in classical Hodgkin lymphoma. *Blood* **2018**, *131*, 2413–2425. [CrossRef] [PubMed]
83. Tiacci, E.; Ladewig, E.; Schiavoni, G.; Penson, A.; Fortini, E.; Pettirossi, V.; Wang, Y.; Rosseto, A.; Venanzi, A.; Vlasevska, S.; et al. Pervasive mutations of JAK-STAT pathway genes in classical Hodgkin lymphoma. *Blood* **2018**, *131*, 2454–2465. [CrossRef] [PubMed]
84. Camus, V.; Stamatoullas, A.; Mareschal, S.; Viailly, P.J.; Sarafan-Vasseur, N.; Bohers, E.; Dubois, S.; Picquenot, J.M.; Ruminy, P.; Maingonnat, C.; et al. Detection and prognostic value of recurrent exportin 1 mutations in tumor and cell-free circulating DNA of patients with classical Hodgkin lymphoma. *Haematologica* **2016**, *101*, 1094–1101. [CrossRef] [PubMed]
85. Alig, S.K.; Shahrokh Esfahani, M.; Garofalo, A.; Li, M.Y.; Rossi, C.; Flerlage, T.; Flerlage, J.E.; Adams, R.; Binkley, M.S.; Shukla, N.; et al. Distinct Hodgkin lymphoma subtypes defined by noninvasive genomic profiling. *Nature* **2024**, *625*, 778–787. [CrossRef] [PubMed]
86. Camus, V.; Viennot, M.; Lequesne, J.; Viailly, P.J.; Bohers, E.; Bessi, L.; Marcq, B.; Etancelin, P.; Dubois, S.; Picquenot, J.M.; et al. Targeted genotyping of circulating tumor DNA for classical Hodgkin lymphoma monitoring: A prospective study. *Haematologica* **2021**, *106*, 154–162. [CrossRef] [PubMed]
87. Desch, A.K.; Hartung, K.; Botzen, A.; Brobeil, A.; Rummel, M.; Kurch, L.; Georgi, T.; Jox, T.; Bielack, S.; Burdach, S.; et al. Genotyping circulating tumor DNA of pediatric Hodgkin lymphoma. *Leukemia* **2020**, *34*, 151–166. [CrossRef] [PubMed]
88. Heger, J.M.; Mammadova, L.; Mattlener, J.; Sobesky, S.; Cirillo, M.; Altmüller, J.; Kirst, E.; Reinke, S.; Klapper, W.; Bröckelmann, P.J.; et al. Circulating Tumor DNA Sequencing for Biologic Classification and Individualized Risk Stratification in Patients With Hodgkin Lymphoma. *J. Clin. Oncol.* **2024**, *42*, 4218–4230. [CrossRef] [PubMed]
89. Paczkowska, J.; Kaszkowiak, M.; Leblanc, M.; Stewart, C.; Herrera, A.; Fernandez del Castillo, J.C.; Castellino, S.; Rutherford, S.; Evens, A.; Davison, K.; et al. Circulating tumor DNA analyses of molecular tumor burden are superior to PET-assessed responses in patients with advanced stage classic Hodgkin lymphoma treated on SWOG S1826. *Blood* **2025**, *146*, 351. [CrossRef]
90. Younes, A.; Gopal, A.K.; Smith, S.E.; Ansell, S.M.; Rosenblatt, J.D.; Savage, K.J.; Ramchandren, R.; Bartlett, N.L.; Cheson, B.D.; de Vos, S.; et al. Results of a pivotal phase II study of brentuximab vedotin for patients with relapsed or refractory Hodgkin's lymphoma. *J. Clin. Oncol.* **2012**, *30*, 2183–2189. [CrossRef] [PubMed]
91. Connors, J.M.; Jurczak, W.; Straus, D.J.; Ansell, S.M.; Kim, W.S.; Gallamini, A.; Younes, A.; Alekseev, S.; Illés, Á.; Picardi, M.; et al. Brentuximab Vedotin with Chemotherapy for Stage III or IV Hodgkin's Lymphoma. *N. Engl. J. Med.* **2018**, *378*, 331–344. [CrossRef] [PubMed]
92. Ansell, S.M.; Radford, J.; Connors, J.M.; Długosz-Danecka, M.; Kim, W.S.; Gallamini, A.; Ramchandren, R.; Friedberg, J.W.; Advani, R.; Hutchings, M.; et al. Overall Survival with Brentuximab Vedotin in Stage III or IV Hodgkin's Lymphoma. *N. Engl. J. Med.* **2022**, *387*, 310–320. [CrossRef] [PubMed]
93. Castellino, S.M.; Li, H.; Herrera, A.F.; LeBlanc, M.; Parsons, S.K.; Unger, J.M.; Punnett, A.; Hodgson, D.; Keller, F.G.; Drachtman, R.A.; et al. Three-Year Follow-Up of Nivolumab-AVD Versus Brentuximab Vedotin-AVD in Adolescents With Advanced-Stage Classic Hodgkin Lymphoma on S1826. *J. Clin. Oncol.* **2026**, *44*, 449–454. [CrossRef] [PubMed]
94. Rutherford, S.C.; Li, H.; Herrera, A.F.; LeBlanc, M.; Ahmed, S.; Davison, K.; Parsons, S.K.; Unger, J.M.; Perry, A.M.; Casulo, C.; et al. Nivolumab-AVD Versus Brentuximab Vedotin-AVD in Older Patients With Advanced-Stage Classic Hodgkin Lymphoma Enrolled on S1826. *J. Clin. Oncol.* **2025**, *43*, 2968–2973. [CrossRef] [PubMed]
95. U.S. Food and Drug Administration. FDA Approves Nivolumab with Chemotherapy for Previously Untreated Hodgkin Lymphoma. 2026. Available online: https://www.fda.gov/drugs/resources-information-approved-drugs/fda-approves-nivolumab-chemotherapy-previously-untreated-hodgkin-lymphoma (accessed on 30 September 2026).

96. Borchmann, P.; Ferdinandus, J.; Schneider, G.; Moccia, A.; Greil, R.; Hertzberg, M.; Schaub, V.; Hüttmann, A.; Keil, F.; Dierlamm, J.; et al. Assessing the efficacy and tolerability of PET-guided BrECADD versus eBEACOPP in advanced-stage, classical Hodgkin lymphoma (HD21): A randomised, multicentre, parallel, open-label, phase 3 trial. *Lancet* **2024**, *404*, 341–352. [CrossRef] [PubMed]
97. European Medicines Agency. Opdivo (Nivolumab): EPAR—Product Information. Available online: https://www.ema.europa.eu/en/medicines/human/EPAR/opdivo (accessed on 9 October 2026).
98. European Medicines Agency. Adcetris (Brentuximab Vedotin): EPAR—Product Information. Available online: https://www.ema.europa.eu/en/medicines/human/EPAR/adcetris (accessed on 9 October 2026).
99. Munir, F.; Hardit, V.; Sheikh, I.N.; AlQahtani, S.; He, J.; Cuglievan, B.; Hosing, C.; Tewari, P.; Khazal, S. Classical Hodgkin Lymphoma: From Past to Future-A Comprehensive Review of Pathophysiology and Therapeutic Advances. *Int. J. Mol. Sci.* **2023**, *24*, 10095. [CrossRef] [PubMed]
100. Plattel, W.J.; van den Berg, A.; Visser, L.; van der Graaf, A.M.; Pruim, J.; Vos, H.; Hepkema, B.; Diepstra, A.; van Imhoff, G.W. Plasma thymus and activation-regulated chemokine as an early response marker in classical Hodgkin's lymphoma. *Haematologica* **2012**, *97*, 410–415. [CrossRef] [PubMed]
101. Guidetti, A.; Mazzocchi, A.; Miceli, R.; Paterno, E.; Taverna, F.; Spina, F.; Crippa, F.; Farina, L.; Corradini, P.; Gianni, A.M.; et al. Early reduction of serum TARC levels may predict for success of ABVD as frontline treatment in patients with Hodgkin Lymphoma. *Leuk. Res.* **2017**, *62*, 91–97. [CrossRef] [PubMed]
102. Hsi, E.D.; Li, H.; Nixon, A.B.; Schöder, H.; Bartlett, N.L.; LeBlanc, M.; Smith, S.; Kahl, B.S.; Leonard, J.P.; Evens, A.M.; et al. Serum levels of TARC, MDC, IL-10, and soluble CD163 in Hodgkin lymphoma: A SWOG S0816 correlative study. *Blood* **2019**, *133*, 1762–1765. [CrossRef] [PubMed]
103. Viviani, S.; Mazzocchi, A.; Pavoni, C.; Taverna, F.; Rossi, A.; Patti, C.; Romano, A.; Trentin, L.; Sorasio, R.; Guidetti, A.; et al. Early serum TARC reduction predicts prognosis in advanced-stage Hodgkin lymphoma patients treated with a PET-adapted strategy. *Hematol. Oncol.* **2020**, *38*, 501–508. [CrossRef] [PubMed]

Disclaimer/Publisher's Note: The statements, opinions and data contained in all publications are solely those of the individual author(s) and contributor(s) and not of MDPI and/or the editor(s). MDPI and/or the editor(s) disclaim responsibility for any injury to people or property resulting from any ideas, methods, instructions or products referred to in the content.